

---

Doctoral Dissertations

Student Theses and Dissertations

---

1973

## A study of gas-surface interactions through sticking coefficient, condensation coefficient and sublimation rate measurements

Charles E. Bryson III

Follow this and additional works at: [https://scholarsmine.mst.edu/doctoral\\_dissertations](https://scholarsmine.mst.edu/doctoral_dissertations)



Part of the [Physics Commons](#)

Department: Physics

---

### Recommended Citation

Bryson, Charles E. III, "A study of gas-surface interactions through sticking coefficient, condensation coefficient and sublimation rate measurements" (1973). *Doctoral Dissertations*. 177.

[https://scholarsmine.mst.edu/doctoral\\_dissertations/177](https://scholarsmine.mst.edu/doctoral_dissertations/177)

This thesis is brought to you by Scholars' Mine, a service of the Missouri S&T Library and Learning Resources. This work is protected by U. S. Copyright Law. Unauthorized use including reproduction for redistribution requires the permission of the copyright holder. For more information, please contact [scholarsmine@mst.edu](mailto:scholarsmine@mst.edu).

A STUDY OF GAS-SURFACE INTERACTIONS THROUGH  
STICKING COEFFICIENT, CONDENSATION COEFFICIENT AND  
SUBLIMATION RATE MEASUREMENTS

BY

CHARLES E. BRYSON, III, 1940-

A DISSERTATION

Presented to the Faculty of the Graduate School of the

UNIVERSITY OF MISSOURI - ROLLA

In Partial Fulfillment of the Requirements for the Degree

DOCTOR OF PHILOSOPHY

in

PHYSICS

1973

T2798  
97 pages  
c.1

Remond P. Peterson  
Advisor

J. Adawi

William R. Snow

Charles O. Goblen

Robert J. Bell

\_\_\_\_\_

PUBLICATION THESIS OPTION <sup>159</sup>

This dissertation has been prepared in the style utilized by Surface Science, The Journal of Vacuum Science and Technology and The Journal of Physical Chemistry. Part I, pages 3-34, has been submitted for publication to Surface Science. Part II, pages 35-67, has been submitted for publication to The Journal of Vacuum Science and Technology. Part III, pages 68-87, has been submitted for publication to The Journal of Physical Chemistry.

## ABSTRACT

The behavior of the sticking coefficient of  $\text{CO}_2$  on an  $\text{H}_2\text{O}$  substrate as a function of time is interpreted in terms of a microscopic nucleation theory. For a substrate temperature near 75 K and an incident flux near  $10^{13}$  molecule  $\text{cm}^{-2}\text{sec}^{-1}$ , a critical cluster size of four molecules and an activation energy of nucleation of  $22 \pm 2.4$  Kcal mole $^{-1}$  is obtained. The analysis treats the nucleation processes as continuous rather than as a discontinuous process at some critical temperature.

In addition the same molecular beam apparatus used for the above experiment was used to measure the condensation coefficient,  $\gamma$ , of  $\text{H}_2\text{O}$ ,  $\text{N}_2\text{O}$ , and  $\text{CO}_2$ , each on a surface of the condensed phase of the same molecule, i.e.,  $\text{H}_2\text{O}$  on  $\text{H}_2\text{O}$ ,  $\text{N}_2\text{O}$  on  $\text{N}_2\text{O}$  and  $\text{CO}_2$  on  $\text{CO}_2$ . This ratio,  $\gamma$ , was observed to be a function of the beam temperature, incident flux, and the time that the surface was exposed to the beam as well as the surface temperature. Problems associated with the definition of  $\gamma$  are discussed in attempts to explain the data. The range of  $\gamma$  observed was 0.5 to 0.995.

As part of these experiments the sublimation rate of  $\text{H}_2\text{O}$ ,  $\text{CO}_2$ ,  $\text{N}_2\text{O}$ , and to have been measured in the temperature range that correspond to vapor pressure between  $10^{-4}$  and  $10^{-9}$  Torr.



## ACKNOWLEDGMENTS

The author wishes to express his appreciation to Dr. L. L. Levenson, Associate Professor of Physics and Senior Investigator at the Space Sciences Research Center (SSRC), for suggesting this project. In addition his advice, assistance, and encouragement in carrying out this work have been sincerely appreciated.

He wishes to thank Dr. R. J. Bell, Professor of Physics, Dr. C. A. Goben, Associate Professor of Electrical Engineering, both Senior Investigators at the SSRC, and Dr. W. R. Snow, Assistant Professor of Physics for their helpful discussions.

The collaboration of Dr. V. Cazcarra, a former student of Dr. Levenson, is recognized with appreciation.

The assistance of the author's wife in preparation of the early drafts of this dissertation is appreciated.

The financial support from the Graduate Center for Materials Research, Graduate Center for Cloud Physics Research, the National Science Foundation, and the Air Force is gratefully acknowledged.

## TABLE OF CONTENTS

	Page
PUBLICATION THESIS OPTION.....	ii
ABSTRACT.....	iii
ACKNOWLEDGMENTS.....	iv
TABLE OF CONTENTS.....	v
LIST OF ILLUSTRATIONS.....	vii
LIST OF TABLES.....	ix
INTRODUCTION.....	1
PART I. Critical Cluster Size Determination from Sticking Coefficient and Flash Desorption Measurements.....	3
ABSTRACT.....	4
INTRODUCTION.....	5
EXPERIMENTAL ARRANGEMENT.....	6
PROCEDURE.....	9
RESULTS.....	11
DISCUSSION.....	15
CONCLUSIONS AND SUMMARY.....	22
ACKNOWLEDGMENTS.....	24
REFERENCES.....	25
PART II. Condensation Coefficient Measurements of H <sub>2</sub> O, N <sub>2</sub> O, and CO <sub>2</sub> .....	35
ABSTRACT.....	36
INTRODUCTION.....	37
EXPERIMENTAL ARRANGEMENT.....	41
PROCEDURE.....	43
RESULTS.....	44
CONCLUSION.....	52

	Page
REFERENCES.....	54
PART III. Sublimation Rates and Vapor Pressures of H <sub>2</sub> O, CO <sub>2</sub> , N <sub>2</sub> O and Xe.....	68
ABSTRACT.....	69
INTRODUCTION.....	70
APPARATUS AND PROCEDURES.....	71
DATA TREATMENT.....	73
RESULTS.....	74
REFERENCES.....	77
VITA.....	88

## LIST OF ILLUSTRATIONS

	Page
PART I.	
1. Molecular Beam Chamber (To Scale).....	28
2. Reflection Coefficient of CO <sub>2</sub> <u>vs</u> Time (T <sub>s</sub> = 72.4 K and 72.9 K).....	29
3. Reflection Coefficient of CO <sub>2</sub> <u>vs</u> Time (T <sub>s</sub> = 73.6 K and 74.4 K).....	30
4. Time Constant, a, <u>vs</u> T <sub>s</sub> <sup>-1</sup> .....	31
5. Reflection Coefficient <u>vs</u> T <sub>s</sub> for T <sub>s</sub> Decreasing with Time.....	32
6. Flux Dependence of T <sub>sp</sub> .....	33
7. Flash Desorption of CO <sub>2</sub> from an H <sub>2</sub> O Surface.....	34
PART II.	
1. System I.....	55
2. System II.....	56
3. Response of Microbalance BM to a step function in flux.....	57
4. Reflection coefficient as a function of reduced flux for H <sub>2</sub> O, System I.....	58
5. Reflection coefficient as a function of reduced flux for CO <sub>2</sub> , System I.....	59
6. Reflection coefficient as a function of reduced flux for N <sub>2</sub> O, T <sub>G</sub> = 130k, System II.....	60
7. Reflection coefficient as a function of reduced flux for N <sub>2</sub> O, T <sub>G</sub> = 150k, System II.....	61
8. Reflection coefficient as a function of reduced flux for N <sub>2</sub> O, T <sub>G</sub> = 170-175k, System II.....	62
9. Reflection coefficient as a function of reduced flux for CO <sub>2</sub> , T <sub>G</sub> = 129k, System II.....	63
10. Reflection coefficient as a function of reduced flux for CO <sub>2</sub> , T <sub>G</sub> = 173k, System II.....	64

	Page
11. Reflection coefficient as a function of reduced flux for $\text{CO}_2$ , $T_G = 188\text{k}$ , System II.....	65
12. Response of microbalance CR to a step function in flux onto the target.....	66
13. Sublimation rate for $\text{N}_2\text{O}$ on a $\text{CO}_2$ substrate and bulk sublimation rate for $\text{CO}_2$ and $\text{N}_2\text{O}$ .....	67
PART III.	
1. Vapor Pressure of $\text{H}_2\text{O}$ <u>vs.</u> Temperature, T.....	84
2. Vapor Pressure of $\text{N}_2\text{O}$ <u>vs.</u> Temperature, T.....	85
3. Vapor Pressure of $\text{CO}_2$ <u>vs.</u> Temperature, T.....	86
4. Vapor Pressure of Xe <u>vs.</u> Temperature, T.....	87

## LIST OF TABLES

	Page
PART I.	
I. Energy of Desorption of $\text{CO}_2$ , $E_s$ , from Flash Desorption Measurement.....	27
PART III.	
I. Vapor Pressure of $\text{H}_2\text{O}$ <u>vs.</u> Temperature, T.....	78
II. Vapor Pressure of $\text{N}_2\text{O}$ <u>vs.</u> Temperature, T.....	79
III. Vapor Pressure of $\text{CO}_2$ <u>vs.</u> Temperature, T.....	80
IV. Vapor Pressure of Xe <u>vs.</u> Temperature, T.....	82
V. Heat of Vaporization and Preexponential for the Data in Tables I-IV.....	83

## INTRODUCTION

The measurements of condensation and sticking coefficient and sublimation rates serve as probes that can partially answer the question of what types of mechanism and what magnitude of interactions exist between gas phase molecules and surfaces. As measured with a molecular beam, both the condensation coefficient and sticking coefficient are the ratio of the amount of material from a beam that stays on a surface to the amount of material incident on the surface. The term condensation coefficient applies in the case where the surface is composed of a condensed phase of the incident material and sticking coefficient applies in the case where the surface is composed of different materials.

Part I of the dissertation describes a study of the sticking coefficient of  $\text{CO}_2$  on a  $\text{H}_2\text{O}$  (ice) surface. The results are discussed in terms of a continuous nucleation model. Part I is the manuscript as submitted for publication to Surface Science.

Part II describes a study of the condensation coefficient of  $\text{H}_2\text{O}$ ,  $\text{N}_2\text{O}$ , and  $\text{CO}_2$ . The results are discussed in terms of several models none of which are entirely satisfactory. This work serves primarily to more completely define the problem, and has been submitted for publication in The Journal of Vacuum Science and Technology.

Part III describes the determination of sublimation rates for  $\text{H}_2\text{O}$ ,  $\text{CO}_2$ ,  $\text{N}_2\text{O}$  and Xe. This particular set of measurements was made as a part of the experimental procedures carried out in Part I and have been submitted to The Journal of Physical Chemistry.



## PART I

Critical Cluster Size Determination from Sticking  
Coefficient and Flash Desorption Measurements

Manuscript to be submitted to Surface Science

## ABSTRACT

The behavior of the sticking coefficient of  $\text{CO}_2$  on an  $\text{H}_2\text{O}$  substrate as a function of time is interpreted in terms of a microscopic nucleation theory. For a substrate temperature near 75 K and an incident flux near  $10^{13}$  molecules  $\text{cm}^{-2}\text{sec}^{-1}$ , a critical cluster size of four molecules and an activation energy of nucleation of  $22 \pm 2.4$  Kcal  $\text{mole}^{-1}$  is obtained. The analysis treats the nucleation processes as a continuous rather than as a discontinuous process at some critical temperature.

## INTRODUCTION

For the purpose of the present investigation, a molecular beam apparatus was used to study the nucleation of  $\text{CO}_2$  on an  $\text{H}_2\text{O}$  surface. A beam of  $\text{CO}_2$  molecules was directed onto an  $\text{H}_2\text{O}$  surface, and the fraction,  $1-\gamma$ , of the molecules that were reflected from the surface was measured<sup>1</sup>. This reflected fraction or reflection coefficient includes both the molecules that are truly reflected and those which are desorbed at a rate higher than the desorption rate that exists in the absence of a beam. As usual, the fraction of the beam that stays on the surface is referred to as the condensation or sometimes the sticking coefficient,  $\gamma$ .

Two types of experiments were performed. Both consisted of measuring  $(1-\gamma)$  as a function of time after the beam was initiated, the time behavior of the beam being approximately a step function. The two methods differed in the way that the temperature of the surface,  $T_s$ , was controlled with time. In the first type of experiment,  $T_s$  and the incident flux,  $D$ , were held constant. These experiments were repeated for various values of  $T_s$ . In the second type of experiment,  $T_s$  was decreased linearly with time in the presence of a beam and the experiment was repeated for different values of  $D$ . With the critical temperature,  $T_s$ , defined as that temperature at which  $(1-\gamma)$  abruptly decreases, this second type of experiment

has been used by several authors to measure  $T_c$  for nucleation as a function of incident flux<sup>(2-4)</sup>. However, for  $\text{CO}_2$  on  $\text{H}_2\text{O}$ , it was found that this assignment of  $T_c$  was ambiguous and was a contradiction to what was observed in the first type of experiment.  $\text{CO}_2$  did accumulate slowly on the  $\text{H}_2\text{O}$  substrate at any higher temperature than could be called critical.

The ambiguity was resolved by a treatment of condensation that is analogous to the treatment of flash desorption by Redhead and others<sup>(5,6)</sup>. In addition, the parameters obtained were interpreted directly in terms of the nucleation rate expression obtained by Walton<sup>(7)</sup> and Lewis<sup>(8)</sup>. We obtained directly the size of the smallest stable cluster and an estimate of the energetics of the nucleation process. This was accomplished without the necessity of an arbitrary definition of critical supersaturation. Also, a heat of desorption of  $\text{CO}_2$  on  $\text{H}_2\text{O}$  was measured by flash desorption, and the value obtained agrees reasonably well with the analysis mentioned above.

#### EXPERIMENTAL ARRANGEMENT

The apparatus used has been described elsewhere but will be briefly reviewed here for convenience<sup>(1)</sup>. Figure 1 shows the experimental chamber and molecular beam tube surrounded by the cryogen reservoir of a cryostat. For these experiments, the cryogen was pumped solid nitrogen

at 50 K. The chamber, shown approximately to scale, was 12.5 cm in diameter and 10 cm deep. It contained three microbalances, the molecular beam nozzle, and a 2.5 cm diameter copper disc that served as a target. The chamber and the nozzle communicated with liquid nitrogen trapped diffusion pumps through tubes which were attached to the top of the cryostat. The pumping system was provided with a capacitor manometer, ionization gauges, and a General Electric monopole spectrometer.

The microbalances were AT-cut quartz crystal resonators 0.3 mm thick and 1.5 cm in diameter<sup>(9)</sup>. They have a dominant resonance nominally at 5 MHz. Changes in frequency,  $\Delta f$ , were related to changes in the number of molecules,  $\Delta N$ , adsorbed per  $\text{cm}^2$  on the microbalances by the expression

$$\Delta N = (1.079 \times 10^{16}) M^{-1} \Delta f, \quad (1)$$

where  $M$  is the gram molecular weight of the adsorbed species. Previous measurements showed that at 50 K at least 99.99 percent of the  $\text{CO}_2$  or  $\text{H}_2\text{O}$  striking it was adsorbed<sup>(10)</sup>. The frequency or, in most cases, the rate of change of frequency with time was measured with a Hewlett-Packard 5360A Computer Counter and associated electronics.

The dimensions of the beam nozzle were chosen so that the spatial distribution of molecules could be calculated from the cosine law for nozzle pressures below

$10^{-1}$  Torr<sup>(9)</sup>. This allowed the rate of arrival of materials on the target disc to be calculated from measurements of the frequency of the microbalance marked BM. The beam tube was provided with a heater and a platinum resistance thermometer. The temperature of the beam for these experiments was  $129 \pm 1$  K.

The copper disc used as a target was machined from pure copper, polished, and then vacuum plated with a film of gold about  $1000 \text{ \AA}$  thick. It was mounted on nylon screws to provide a small thermal leak to the cryogenic bath. Resistance thermometers, germanium and platinum, which were placed in cavities machined into the disc, allowed the temperature to be determined to within 0.1 K. A comparison of the two thermometers with each other and with temperatures determined by the vapor pressure of liquid nitrogen near 77 K and solid Argon near 50 K confirmed this precision.

In addition, a movable shutter was provided that could shield the target from the beam to allow the beam flux to be stabilized before exposure.

The  $\text{H}_2\text{O}$  used for these experiments was doubly distilled and then outgassed at 100 C for 10 minutes before evacuation. Subsequent mass analysis showed a  $\text{CO}_2$  content of approximately 0.5 mole percent. The high purity  $\text{CO}_2$ , commercially available, showed no measurable impurity with the mass spectrometer. The sensitivity was such that an impurity of 0.01 percent  $\text{O}_2$  would have been detectable.

## PROCEDURE

The H<sub>2</sub>O surface was prepared by heating the beam to 270 K and introducing H<sub>2</sub>O vapor at a nozzle pressure of 10<sup>-2</sup> Torr. This gave an incident flux near 10<sup>15</sup> molecules cm<sup>-2</sup>s<sup>-1</sup>. The beam was left on until approximately 5 x 10<sup>20</sup> molecules cm<sup>-2</sup> were deposited on the top of the target disc. The disc was heated to 100 K for the deposition and then heated to 150 K briefly to anneal the H<sub>2</sub>O film. After each exposure of the surface to CO<sub>2</sub>, the surface was again heated to approximately 150 K. This procedure resulted in about 2.00 x 10<sup>17</sup> molecules cm<sup>-2</sup> of H<sub>2</sub>O being sublimated from the disc, thereby leaving a reproducible H<sub>2</sub>O surface. The disc was then protected by the shutter and allowed to cool.

The first type of experiment was carried out by adjusting the heat to the disc until the temperature was stable at the desired temperature, adjusting the pressure of CO<sub>2</sub> in the beam tube to give the desired flux, and then opening the shutter. The flux was held to a given value to within  $\pm$  5 percent. The material reflected and/or desorbed from the H<sub>2</sub>O surface was monitored with the microbalance marked CR in Fig. 1. The reflection coefficient, (1- $\gamma$ ), was calculated from Eq. (2) where  $\dot{f}_{CR}$  is the rate of change of the frequency of the microbalance CR,  $\dot{f}_{BM}$  is the rate of change of the microbalances marked BM, and  $\bar{K}$  is a geometric factor.

$$(1-\gamma) = \bar{K} \dot{f}_{CR} (\dot{f}_{BM})^{-1} \quad (2)$$

The factor  $\bar{K}$  was measured experimentally with an accuracy of  $\pm 4$  percent by establishing  $T_s$  high enough so that there was a negligible amount of condensation, i.e.,  $\gamma = 0$ . This value of  $\bar{K}$  agreed with that calculated on the basis of a perfectly diffuse reflection of molecules from the copper disc and on a basis of appropriate measurements of the geometry<sup>(11)</sup>. Implicit in the use of this value of  $\bar{K}$  for calculating  $(1-\gamma)$  was the assumption that the spatial distribution of molecules leaving the surface of the target disc remained constant throughout the experiment.

The second experiment was performed in a similar manner except that before the beam was established the copper disc was raised to a higher temperature,  $T_0$ , and then allowed to cool after the shutter was opened.

After each exposure of the  $H_2O$  surface to  $CO_2$ , the copper block was heated slowly, and the desorption of material was recorded with the microbalance CR. The temperature was increased linearly with time until a temperature of 150 K was obtained. The copper block was then allowed to cool to the temperature of the next adsorption experiment. The measured rate of heating and the temperature at which the maximum desorption rate was reached were used to calculate the activation energy of  $CO_2$  desorption as described later.



## RESULTS

For the experiments where  $T_s$  was held constant to within  $\pm 0.05$  K,  $(1-\gamma)$  was observed to rise rapidly from near zero to approximately unity and then to decay slowly back toward zero in an exponential manner. The initial rise corresponds to the adsorption of an initial population of molecules on the surface prior to the beginning of appreciable nucleation. The value of this initial population was obtained by integrating the product of the flux,  $D$ , and the instantaneous value of  $\gamma$  to the time at which  $(1-\gamma)$  reached its maximum value. Typical values obtained were on the order of  $10^{15}$  molecules  $\text{cm}^{-2}$ . This point was discussed in more detail in an earlier paper<sup>(1)</sup>. The exponential decay part of the  $(1-\gamma)$  vs time behavior can be characterized by a decay time constant,  $a$ . Figures 2 and 3 show the behavior of  $\log_{10} (1-\gamma)$  vs time for  $T_s = 72.4$  K, 72.9 K, and 73.6 K, and 74.4 K. The time constant,  $a$ , was calculated from the data taken for the three lower temperatures. The data are described by

$$(1-\gamma) = (1-\gamma_0) \exp[-t/a], \quad (3)$$

where  $\gamma_0$  is the initial value of  $\gamma$ . The data for 74.4 K were treated by fitting the data to a straight line on a linear plot. In this treatment, the straight line represents the first two terms in a series expansion.

The experiment was also performed at  $T_s = 75.5$  K, but the change in  $(1-\gamma)$  with time after rising to near unity was too small to measure reliably. For this case, the constant  $a$  was obtained by measuring the area under the subsequent desorption curve and equating this amount of material to what would be expected by integrating the product of the incident flux and the condensation coefficient. After an exposure of  $9.12 \times 10^3$  seconds with  $n_1 = 7.74 \times 10^{13}$  molecules  $\text{cm}^{-2}\text{sec}^{-1}$ ,  $2.59 \times 10^{16}$  molecules  $\text{cm}^{-2}$  were desorbed.

Figure 4 is a plot of  $\log_{10} \underline{vs} 1000/T_s$  for the data just described. These data are approximately described by the line shown which represents

$$a = a_0 \exp\left[-\frac{E_a}{RT_s}\right], \quad (4)$$

where  $E_a = 22 \text{ Kcal mole}^{-1} \pm 2.4 \text{ Kcal mole}^{-1}$ , and  $a_0 = 8.9 \times 10^{70} \text{ sec}$ .

The dotted line in Fig. 5 is a representative curve showing the behavior of  $(1-\gamma)$  as a function of time and  $T_s$  for the experiment, where  $T_s$  decreased with time. The same flux as in the experiment described above was used. The solid line is theoretical and will be described later. This type of experiment has been used by several other experimenters to determine the critical temperature for nucleation at a given flux<sup>(2-4)</sup>. The critical temperature is normally defined to be that temperature at which

the rate of the material leaving the surface decreases sharply.

For the case of  $\text{CO}_2$  on  $\text{H}_2\text{O}$ , the above mentioned assignment of a critical temperature was ambiguous. Specifically,  $(1-\gamma)$  was observed to decrease gradually with temperature as shown by the data point and dotted curve in Fig. 5. In addition, the first type of experiment indicated that condensation was occurring at a finite rate at 75.5 K, while in the second type of experiment,  $(1-\gamma)$  had not really changed more than the confidence level of the experiment by the time  $T_s$  had fallen to 75.5 K. This implies that a critical temperature can be defined only in terms of the signal-to-noise ratio of the experiment. Here, we found the inflection point to be the most reproducible point on the  $(1-\gamma)$  vs  $T_s$  curve. This temperature, which we call  $T_{sp}$ , was observed to vary with the incident flux,  $D$ . The data, shown in Fig. 6, approximately fit the line shown, which is described by the equation

$$D = c \exp\left[-\frac{E_b}{RT_{sp}}\right], \quad (5)$$

where  $c = 9.58 \times 10^{26}$ , and  $E_b = 4.38 \pm 0.04$  Kcal mole<sup>-1</sup>.

After each adsorption experiment, the surface was heated and the  $\text{CO}_2$  desorbed. The desorption was observed to give rise to a single asymmetric peak in the frequency vs  $T_s$  curve. A typical desorption curve is shown in Fig. 7. If the energy of desorption,  $E_s$ , is independent of the

coverage and if the order of the desorption process is known, then the temperature at which the peak occurs,  $T_p$ , can be related to  $E_s$  <sup>(5)</sup>. Assuming the  $E_s$  is independent of coverage and  $T_s$  varies linearly with time, then

$$\frac{E_s}{RT_p} = \frac{\nu}{\beta} \exp\left[-\frac{E_s}{RT_p}\right] \quad (6)$$

where  $\nu$  is the vibrational frequency factor, and  $\beta$  is temperature sweep rate.

Table I is a tabulation of the  $E_s$  values, which we found by using this technique and by assuming  $\nu = 10^{13}$  ( $\text{sec}^{-1}$ ). The average value of  $E_s$  is  $6007 \text{ cal mole}^{-1}$ . Its standard deviation is  $122 \text{ cal mole}^{-1}$ . The coverages given are in terms of  $N$ , the number of molecules per  $\text{cm}^2$  on the geometric surface.

Previous measurements of the specific surfaces (apparent area per unit geometric area) of gold deposits and  $\text{H}_2\text{O}$  deposits have yielded values near 2.8 for the gold and much larger for  $\text{H}_2\text{O}$ . The specific surface was determined from adsorption isotherms of argon through the isotherm equation of Brunauer, et al. <sup>(12)</sup>. The values for the  $\text{H}_2\text{O}$  deposits were obtained without annealing, so they are unreliable for our purposes. They are mentioned only to point out that the specific surface is probably greater than 2.8 and possibly much greater than 2.8. With this uncertainty in specific surface, it is not readily apparent

whether the desorption of  $\text{CO}_2$  measured is from  $\text{CO}_2$  clusters or from the  $\text{H}_2\text{O}$  surface. In the analysis that follows, it will be apparent that the former case is more probable.

#### DISCUSSION

In the following discussion, an analysis procedure is presented that allows one to relate the parameters obtained in the first type of experiment,  $E_a$  and  $a_0$ , to the parameters obtained in the second type of experiment,  $E_b$  and  $T_{sp}$ . In addition, the general shape of the curve  $(1-\gamma)$  vs  $T_s$  can be explained. These experimental parameters are then discussed in terms of an atomistic nucleation theory from which the critical cluster size is obtained.

We begin by treating  $(1-\gamma)$  in a manner similar to the way in which Redhead<sup>(5)</sup> treated coverage during desorption. It is assumed that a constant population density of monomers on the surface is established in a short time interval after the beam is turned on and that subsequent changes in  $(1-\gamma)$  can be described by the equations

$$\frac{d(1-\gamma)}{dt} = \frac{-1}{a}(1-\gamma) \quad (7)$$

and

$$a = a_0 \exp\left[\frac{-E_a}{RT_s}\right] \quad (4)$$

suggested by the first type of experiment. The second type of experiment consists of letting  $T_s$  decrease linearly with time,  $t$ , as

$$T_s = T_o - bt, \quad (8)$$

where  $b$  is the temperature sweep rate.

The above equations can be combined and integrated. The integration is performed by noting the identity

$$\frac{d}{dT_s} [T_s^2 \exp(\frac{E}{RT_s})] \equiv -\frac{E}{R} \exp(\frac{E}{RT_s}) (1 + \frac{2RT_s}{E}) \quad (9)$$

and approximation  $2RbE^{-1} \ll 1$ . If one takes the initial condition to be  $(1-\gamma) = (1-\gamma_o)$  at  $t = 0$ , then for  $T_s \leq 0.9 T_o$

$$(1-\gamma) = (1-\gamma_o) \left[ \frac{-1}{a_o b} \frac{R}{E_a} T_s^2 \exp\left[\frac{E_a}{RT_s}\right] \right]. \quad (10)$$

The solid line in Fig. 5 was obtained by using the values of  $a_o$  and  $E_a$  from the first type of experiment and by adjusting  $\gamma_o$  to fit the data. As seen in Fig. 5, the agreement is excellent considering the uncertainty in  $E_a$ .

The inflection point,  $T_{sp}$ , can be obtained by taking the second derivative of  $(1-\gamma)$  in Eq. (10) with respect to  $T_s$  and setting it equal to zero. The result is

$$\frac{E_a}{RT_{sp}^2} = \frac{1}{a_o b} \exp\left[\frac{E_a}{RT_{sp}}\right]. \quad (11)$$

This equation is similar to Eq. (6) and gives a nearly linear relationship between  $E_a$  and  $T_{sp}$ .

By analogy with the work of Redhead<sup>(5)</sup>,  $T_{sp}$  occurs when  $(1-\gamma) = (1-\gamma_0)e^{-1}$ . Equation (11) can be rearranged to give  $a_0$  as a function of  $T_{sp}$ , i.e.,

$$a_0 = \frac{R}{bE_a} T_{sp}^2 \exp\left[\frac{E_a}{RT_{sp}}\right]. \quad (12)$$

Note that in Eq. (5), we already have an experimentally determined relationship between  $D$  and  $T_{sp}$ . It now remains to relate  $a_0$  to  $D$ .

In an earlier paper<sup>(1)</sup>, a model for relating the reflection coefficient,  $(1-\gamma)$ , and the fractional area of the surface covered by clusters,  $A_c$  was discussed. This model works for gases, such as  $CO_2$  on  $H_2O$ , gold on rock salt<sup>(13)</sup>, where there is a significant difference in trapping probability for the incident material on the substrate and for the incident material on itself. In these cases,  $\gamma$  can be considered to be a sum, i.e.,

$$\gamma = \alpha_1 A_c + \alpha_2 (1-A_c) \quad (13)$$

where  $\alpha_1$  is the condensation coefficient for the incident material on a cluster, and  $\alpha_2$  is the sticking coefficient on the fraction  $(1-A_c)$  of the substrate which is partially covered with monomers. The measurements of  $(1-\gamma)$  just after a beam of  $CO_2$  begins to hit a fresh, bare  $H_2O$  surface would suggest that  $\alpha_2$  is near unity when the

monomer population density is low. However, once a layer of monomers builds up to a steady state value,  $\alpha_2$  is near 0.04<sup>(1)</sup>. Measurements of  $\gamma$  for a high coverage of CO<sub>2</sub>, presumably a measure of  $\alpha_1$  gives values of  $\alpha$  greater than 0.95 for the fluxes and temperatures used<sup>(10)</sup>. In this case, the behavior of  $\gamma$  with time, as represented by  $(1-\gamma)$ , effectively represents the behavior of  $A_c$  with time.

After the beam is turned on and after the brief prenucleation period, the change in  $A_c$  with time can be described by the differential equation<sup>(14)</sup>

$$dA_c/dt = K_1(1-A_c) + K_2(A_c). \quad (14)$$

The last term represents the growth of the clusters wherein the molecules impinge directly onto existing clusters. In conformance with the practice of most workers<sup>(1)</sup>, the last term will be neglected. The first term on the right represents the mechanisms of growth of  $A_c$  from molecules weakly adsorbed on the surface not already covered by clusters. These mechanisms include the nucleation of new clusters and the growth of existing clusters by molecules diffusing onto them. The desorption of material from clusters already formed can be neglected because the temperature  $T_s$  is too low for rapid desorption. Likewise, the rate of diffusion of molecules out of a cluster is small. By comparing the above differential equation for  $A_c$  with the one implied by the experiment for



$(1-\gamma)$ , i.e., Eq. (7), one has

$$K_1 = 1/a. \quad (15)$$

In the authors' previous work<sup>(1)</sup>,  $K_1$  was tentatively considered to have resulted mainly from the diffusion of adsorbed molecules from existing clusters. However, this implies that  $K_1$  would be proportional to  $D$ , and this conclusion is not consistent with the relationship between  $a_0$  and  $T_{sp}$  and the data represented by Eq. (5). If instead, we assume, as did Lewis and Campbell<sup>(15)</sup>, that the area covered by clusters is changed mainly because of the formation of new clusters, then

$$K_1 = I\tilde{a}_n \quad (16)$$

where  $I$  is the nucleation rate in number of clusters  $\text{cm}^2\text{-sec}$ , and  $\tilde{a}_n$  is some average cluster size in  $\text{cm}^2$ . This size will probably be bigger than the least stable size. In a review of nucleation by Morris<sup>(16)</sup>, it was shown for the situation where the monomer density is desorption determined that

$$I = C_n (D)^n \exp\left[-\frac{E_n}{RT_s}\right] \quad (17)$$

where  $n$  is the number of molecules in the least stable size cluster,  $C_n$  is a constant depending on  $n$ , and  $E_n$  is the activation energy of the nucleation process. This condition yields

$$a = \tilde{a}_n^{-1} (D^{-n}) \exp\left[\frac{-E_n}{RT_s}\right]. \quad (18)$$

Note that  $E_a = E_n$ .

By inspection of Eqs. (17) and (4), one has

$$\alpha_o \sim D^{-n}. \quad (19)$$

By combining this last expression with Eq. (12), which relates  $a_o$  and  $T_{sp}$ , one obtains

$$D^{-n} = T_{sp}^2 C' \exp\left[\frac{E_a}{RT_{sp}}\right] \quad (20)$$

or

$$D = C'' T_{sp}^{-2/n} \exp\left[\frac{-E_a}{nRT_{sp}}\right] \quad (21)$$

where  $C'$  and  $C''$  are collected constants. It is implied that  $\alpha_2$  remains constant throughout. Recalling Eq. (5), the experimental relation between  $D$  and  $T_{sp}$  and treating the  $T_{sp}^{-2/n}$  in the pre-exponential term of Eq. (21) as a constant leads to

$$n = \frac{E_a}{E_b} \quad (22)$$

For the data reported here,  $n = 5.1 \pm 0.5$ .

The nucleation rate as derived by Walton<sup>(7)</sup> shows that  $E_n$  is the sum

$$E_n = nE_\alpha + E_i - E_d \quad (23)$$

where  $E_i$  is the binding energy of a cluster of  $i$  molecules,  $E_d$  is the energy of diffusion, and  $E_\alpha$  is the desorption energy of the adsorbed molecules on the substrate. Here  $i$  is the number of molecules in the critical size cluster;  $i = n-1$ .

A simple estimate of  $E_i$  can be made by assuming that the cluster takes on the same crystalline form as the bulk material and by equating  $E_i$  to an integer multiple of an average bond strength<sup>(8)</sup>. For  $\text{CO}_2$ , which has a simple cubic lattice<sup>(17)</sup>, and  $i = 4$ ,  $E_i \approx 4 E_\beta$  where  $E_\beta$  is the pair bond energy of  $\text{CO}_2$ . If one further assumes  $E_\alpha = 3 E_d$  then

$$E_n = 5 E_\alpha + 4 E_\beta - 1/3 E_\alpha = 14/3 E_\alpha + 4 E_\beta \quad (24)$$

If one takes  $E_\beta$  to be  $0.4 E_s$  -- which implies that in the flash desorption above, the  $\text{CO}_2$  was sublimating predominantly from the clusters and not from the substrate -- then  $E_\alpha = 2.66 \text{ Kcal mole}^{-1}$ .

An alternate assumption is to consider the flash desorption experiment to be a direct measure of  $E_\alpha$ . Then,  $E_\beta$  is negative for the critical cluster shape assumed. Because a negative  $E_\beta$  is not physically meaningful, one can conclude that the desorption energy,  $E_\alpha$  of  $\text{CO}_2$  on  $\text{H}_2\text{O}$ , will be near  $2.66 \text{ Kcal mole}^{-1}$  and the pair bond strength,  $E_\beta$ , is  $2.4 \text{ Kcal mole}^{-1}$ . This value of  $E_\alpha$  was out of the range accessible for flash desorption with the apparatus which was used but will be investigated later.

## CONCLUSIONS AND SUMMARY

On the basis of the data and analysis, it can be concluded that for  $\text{CO}_2$  incident on an  $\text{H}_2\text{O}$  surface the  $\text{CO}_2$  nucleates with a critical cluster size of four molecules. This is for surface temperatures near 74 K and incident fluxes near  $10^{13}$  molecules  $\text{cm}^{-2}\text{sec}^{-1}$ . In addition, the activation energy of nucleation,  $E_n$ , is estimated to be 22 Kcal  $\text{mole}^{-1}$ . By using an atomistic model for the nucleation rate and the flash desorption data of  $\text{CO}_2$  from the  $\text{H}_2\text{O}$  surface, the  $\text{CO}_2$ - $\text{CO}_2$  bond strength can be estimated to be approximately 2.66 Kcal  $\text{mole}^{-1}$  and the energy of adsorption of  $\text{CO}_2$  on  $\text{H}_2\text{O}$  to be near 2.4 Kcal  $\text{mole}^{-1}$ .

A simple model is used to relate reflection coefficient measurements to the fractional area of the surface covered with clusters,  $A_c$ , and to analyze the time dependence of  $A_c$ . There are two aspects of this model that require further comment.

First, the condensation coefficient,  $\alpha_2$ , used to describe the rate at which material is adsorbed onto the surface between clusters, is required to be small and near constant. While  $A_c$  is small,  $\alpha_2$  is expected to be small because most of the molecules are expected to desorb rather than to be captured in clusters. This is observed experimentally; however, as  $A_c$  increases, this situation should change due to depletion of the monomers near the clusters.

Effects of these changes were not seen, because the time constant associated with the changes in  $A_c$  with time did not vary measurably during any individual experiment. Some minor changes in the time constant were noted, but most likely, these reflect small, 3 to 5 percent, variations of pressure that are grossly magnified because the time constant is proportional to  $D^5$ . A possible reason that changes in the time constant did not show up is that any increase in  $\alpha_2$  tends to be offset by saturation effects in the nucleation density. These saturation effects, which are also caused by depletion of monomers near the clusters, and the coalescence are described by Stowell and Hutchinson<sup>(18)</sup> and by Rutledge and Stowell<sup>(19)</sup>. Although a direct comparison of their calculations and the data obtained in the present investigation is difficult because of the simplifying assumptions, their results do indicate that near  $A_c = 0.1$  saturation effects should be appreciable. After the equipment, which was used in the present study, is modified for better beam flux control so that more precise measurements can be made, a more exact analysis may be justified.

The second aspect to consider is that the nucleation expressions used are essentially atomistic in nature. The internal structure of the molecules used here did not noticeably enter into the considerations. The word molecule is simple substituted for atom. It will be of interest to look for effects attributable to the internal

modes of the molecules. This will be done in future experiments by varying the temperature of the incident beam.

#### ACKNOWLEDGMENTS

The authors are grateful for support from the Atmospheric Science Section of the National Science Foundation under Grant GA 13948. Helpful discussions with Drs. Barbara Hale and Patricia Plummer are greatly appreciated.

## REFERENCES

1. V. Cazcarra, C. E. Bryson, III, and L. L. Levenson, *J. Vac. Sci. and Tech.* 10, 148 (1973).
2. R. J. H. Voorhoeve, R. S. Wagner, and J. N. Caride, *J. Vac. Sci. and Tech.* 9, 780 (1971).
3. J. B. Hudson, and J. S. Sandejas, *J. Vac. Sci. and Tech.* 4, 230 (1967).
4. J. H. Heald, Jr., and R. F. Brown, AECD-TR-68-110 (September 1968).
5. P. A. Redhead, *Vacuum* 12, 203 (July 1962).
6. T. W. Reynolds, NASA TN D-4789 CFSTI, Springfield, VA. (1968).
7. D. Walton, *J. Chem. Phys.* 37, 2182 (1962).
8. B. Lewis, *Surface Sci.* 21, 289 (1970).
9. L. L. Levenson, *Suplemento al Nuevo Cimento*, Ser. 1. 5, 321 (1967).
10. C. E. Bryson, III, V. Cazcarra, M. Chouarain, and L. L. Levenson, *J. Vac. Sci. and Tech.* 4, 557 (1972).
11. C. E. Bryson, III, V. Cazcarra, and L. L. Levenson, *J. Vac. Sci. and Tech.* 10, 310 (1973).
12. S. Brunauer, P. H. Emmett, and E. Teller, *J. Am. Chem. Soc.* 60, 309 (1938).
13. C. A. O. Henning, *Surface Sci.* 9, 277-295 (1968).
14. T. N. Rhodin, W. H. Orr, and D. Walton, "Nucleation and Growth of Oxide on Metals," in Processus de Nucleation dans les Reactions des Gaz sur les Reactions des Gaz sur les Metaux et Problemes Connexes, Colloques Internationaux du Centre National de la Recherche Scientifique, No. 122, Paris 10-15 June, 1963. Editions du C.N.R.S., Paris 1965.
15. B. Lewis and D. S. Campbell, *J. Vac. Sci. and Tech.* 4, 209 (1967).
16. W. L. Morris, Ph.D. Dissertation, Northwestern U. (1968).

17. A. Ron and O. Schnepp, J. Chem. Phys. 46, 3991 (1967).
18. M. J. Stowell and T. E. Hutchinson, Thin Solid Films 8, 41 (1971).
19. V. J. Routledge and M. J. Stowell, Thin Solid Films 6, 407 (1970).



TABLE 1

$T_p$ °K	$\beta$ °K/sec	$E_s$ cal/mole	$N \times 10^{-15}$ mol/cm <sup>2</sup>
86.7	0.024	5956	24.4
84.2	0.024	5774	18.4
84.8	0.008	5997	3.84
86.7	0.016	6026	12.32
88.5	0.012	6209	25.1
86.7	0.022	5973	41.9
88.3	0.024	6071	85.9
90.0	0.024	6195	167.0
86.0	0.022	5919	34.7
83.2	0.005	5951	25.8

$$\langle E_s \rangle = 6007$$

$$\sigma_{E_s} = 122$$

Energy of Desorption of CO<sub>2</sub>,  $E_s$ , from Flash  
Desorption Measurement

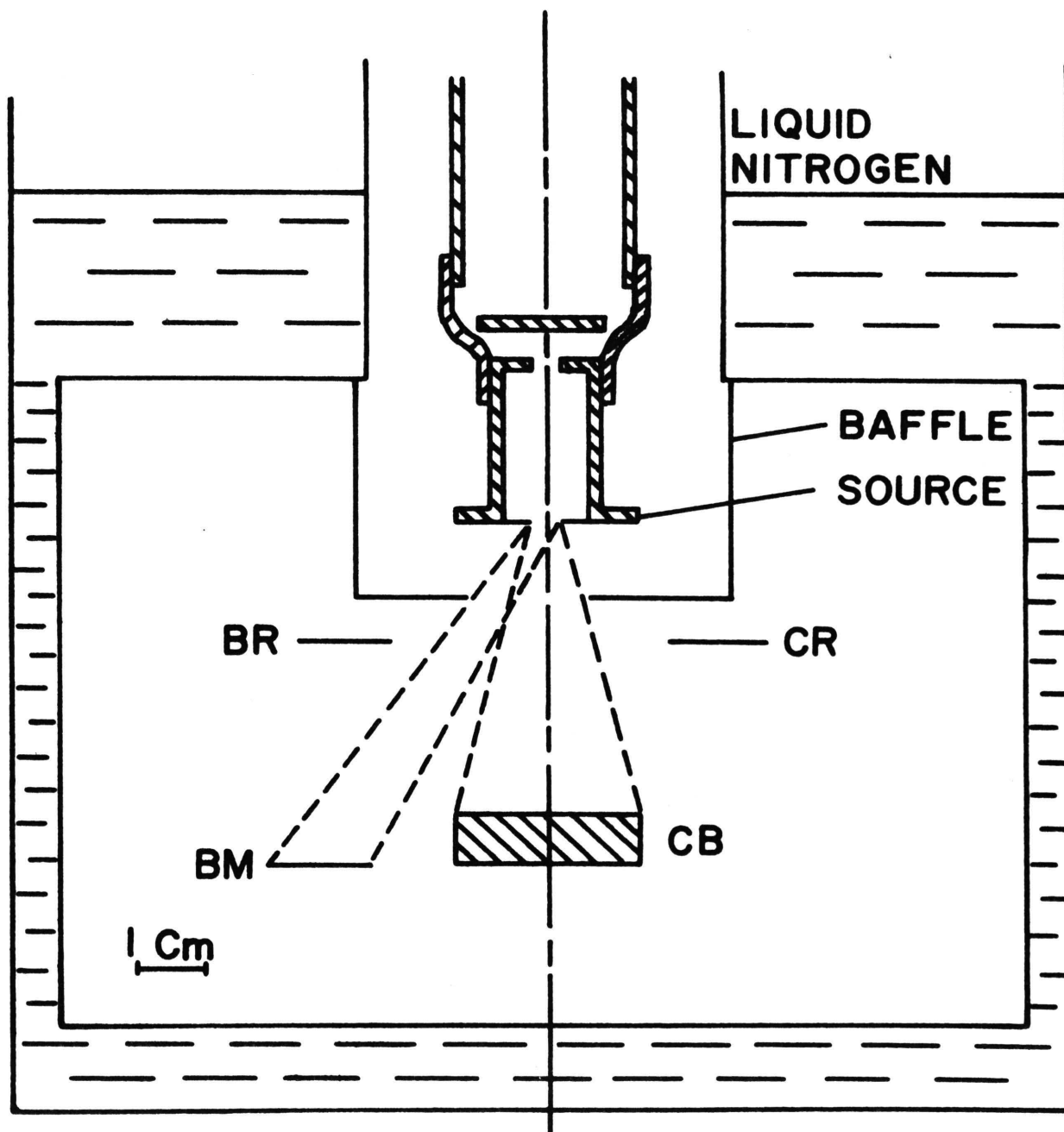


Figure 1. Molecular Beam Chamber (To Scale)

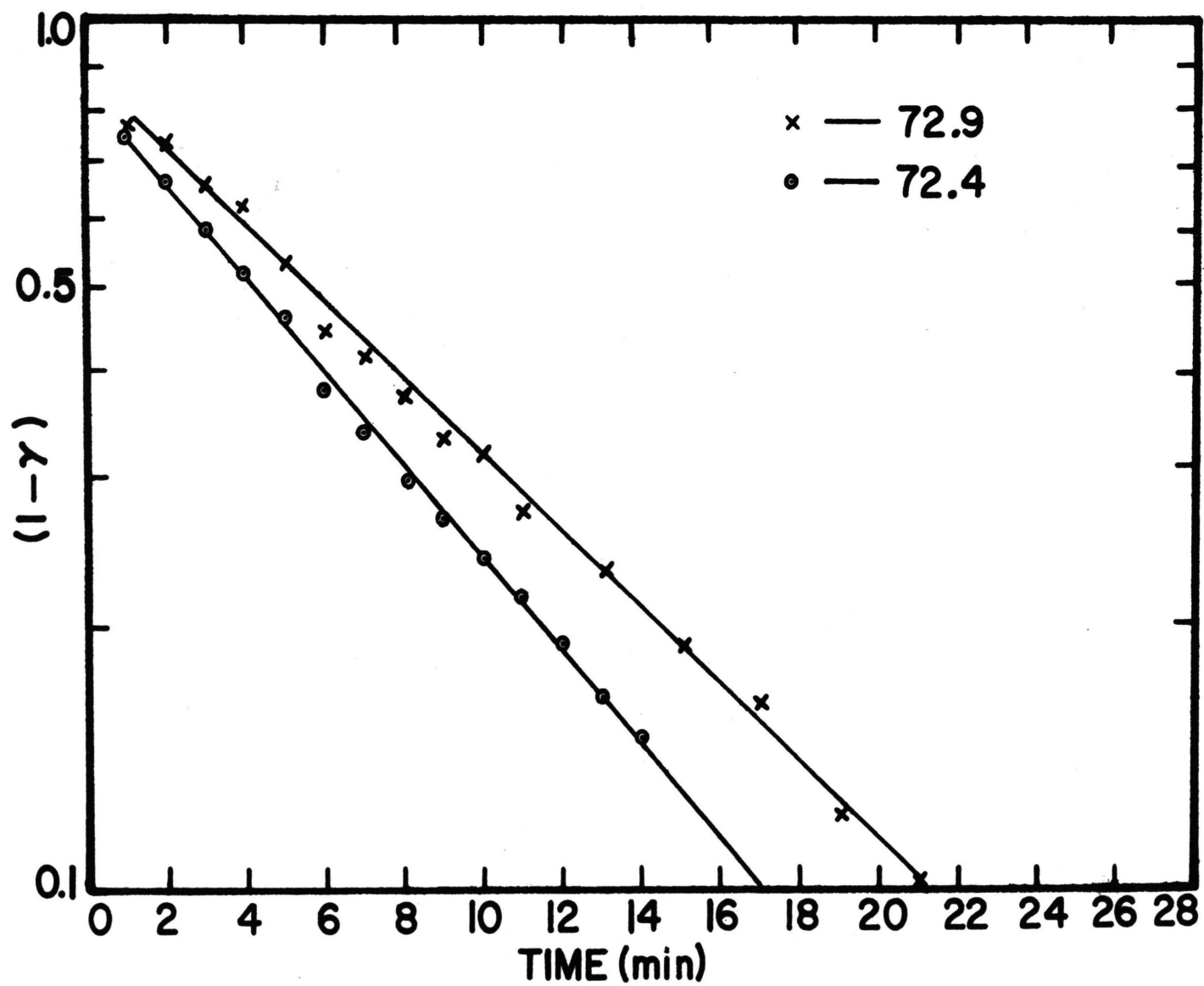


Figure 2. Reflection Coefficient of  $\text{CO}_2$  vs Time ( $T_s = 72.4$  K and  $72.9$  K)

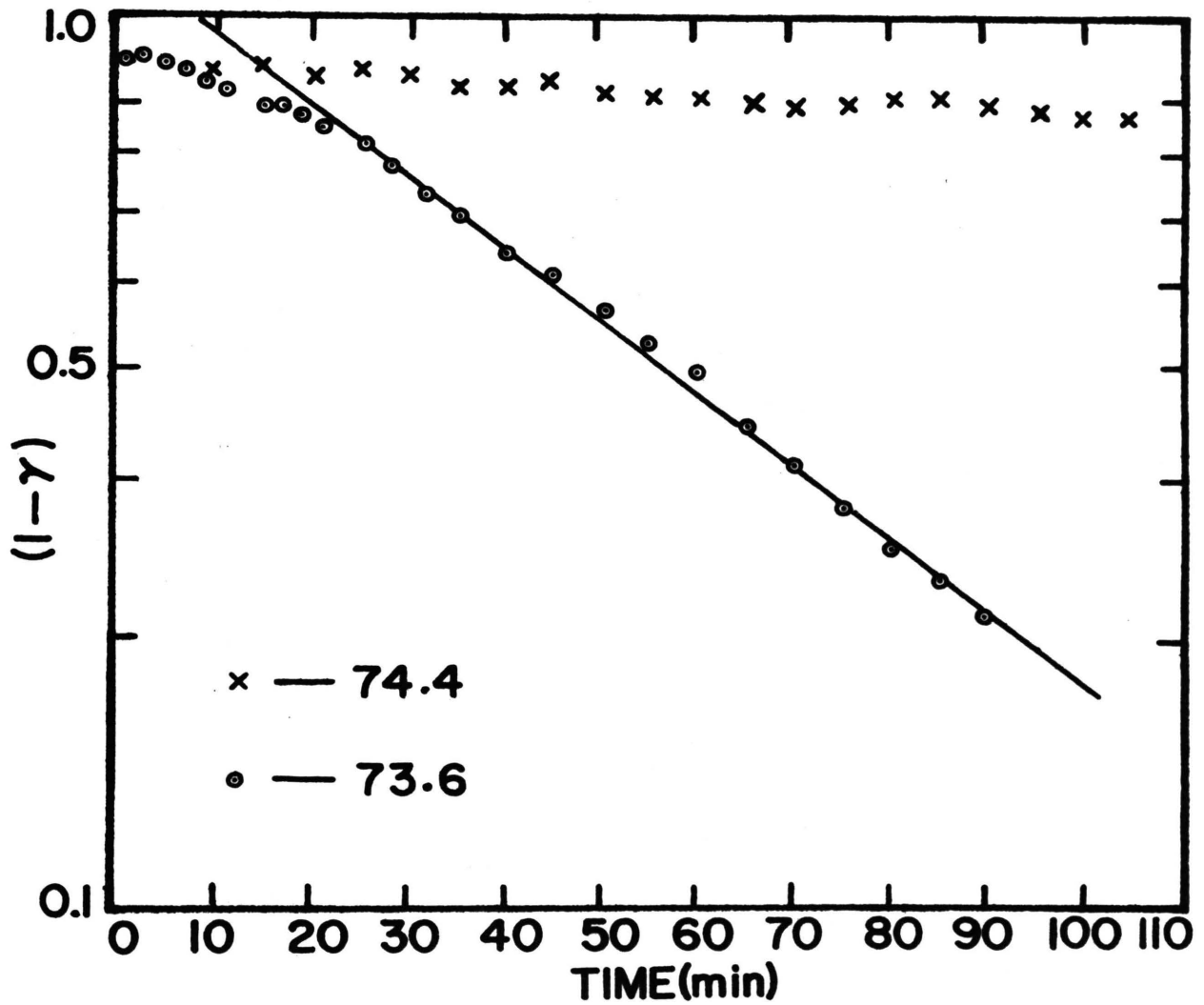


Figure 3. Reflection Coefficient of  $\text{CO}_2$  vs Time  
( $T_s = 73.6 \text{ K}$  and  $74.4 \text{ K}$ )

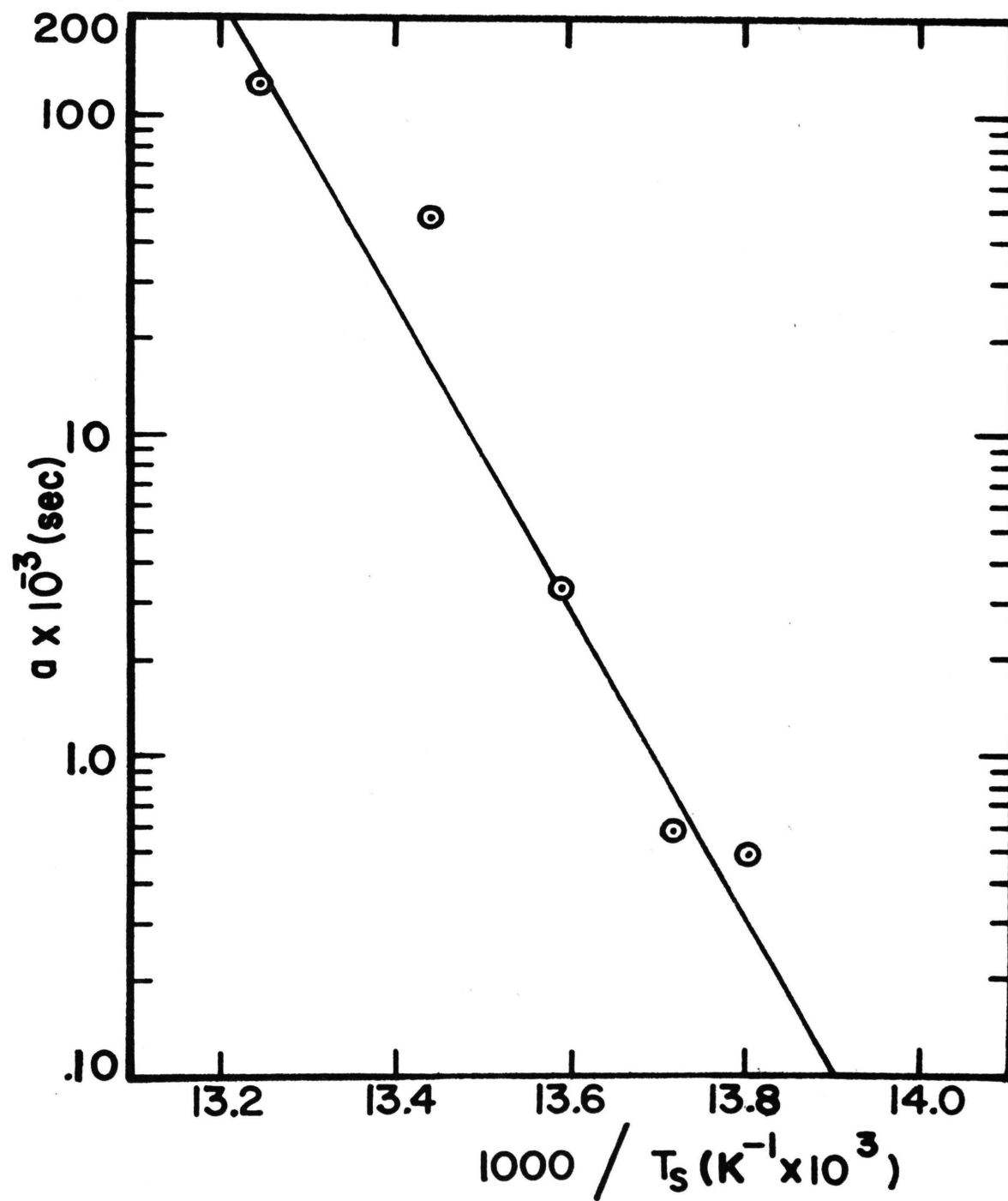


Figure 4. Time Constant,  $a$ , vs  $T_s^{-1}$

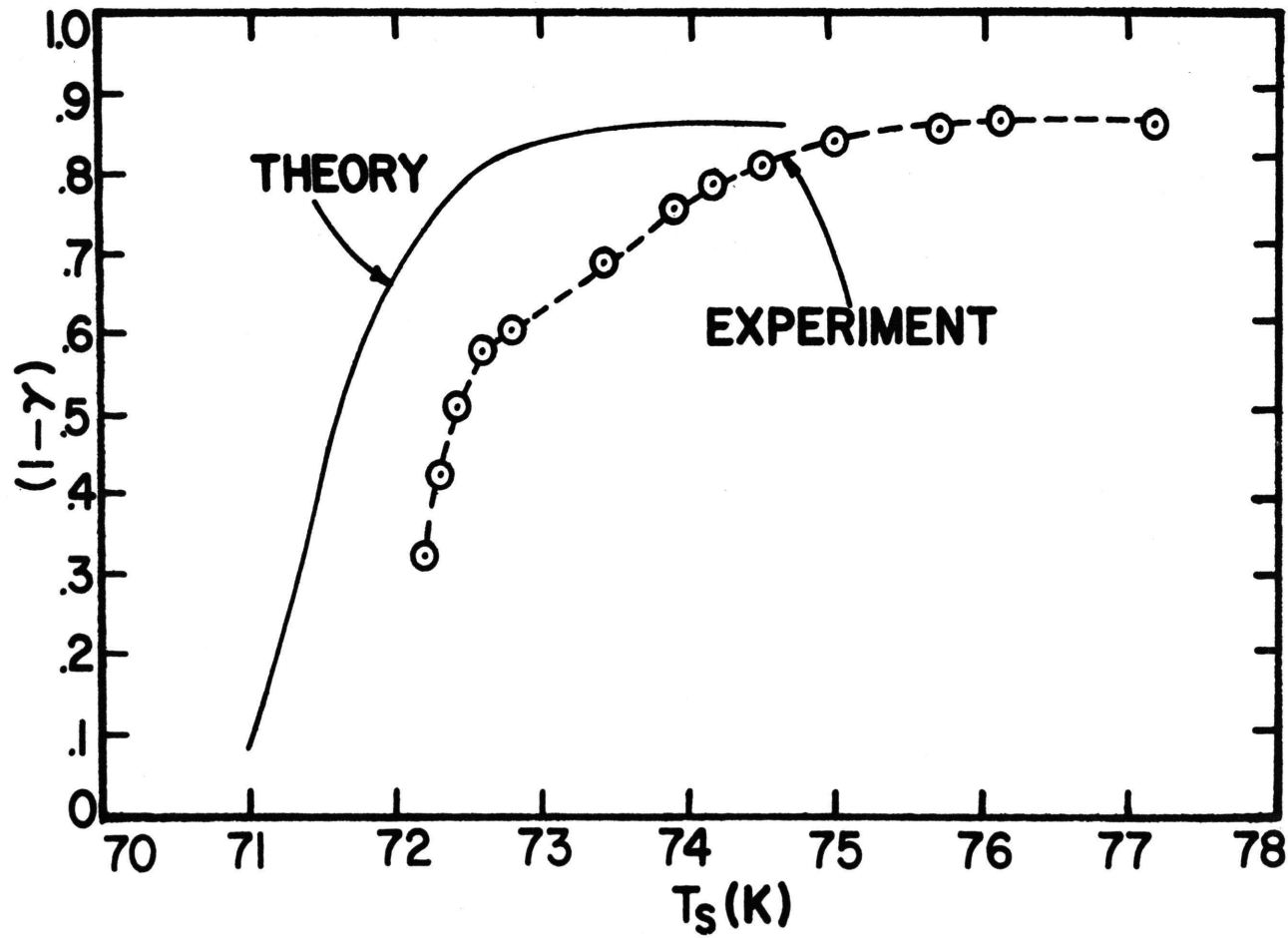


Figure 5. Reflection Coefficient vs  $T_s$  for  $T_s$  Decreasing with Time

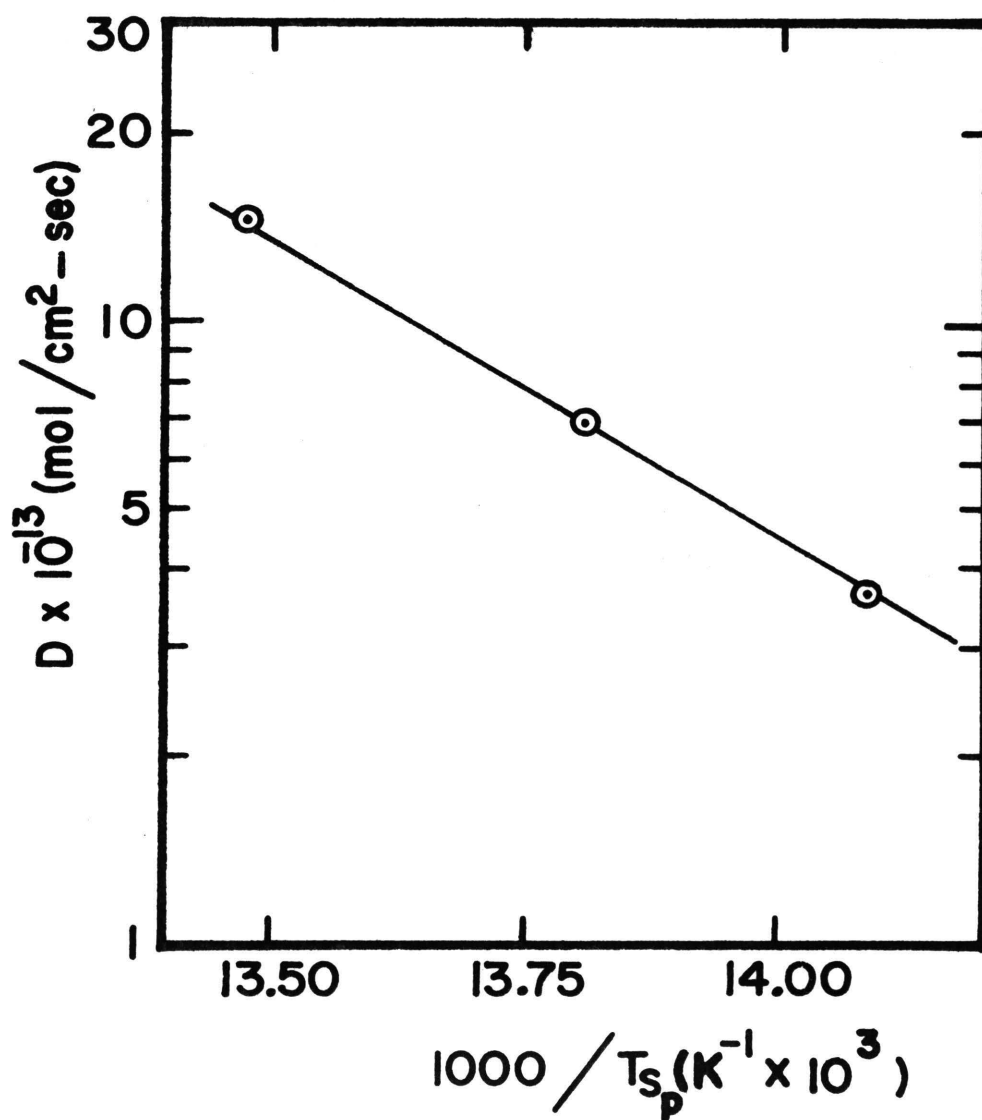


Figure 6. Flux Dependence of  $T_{sp}$

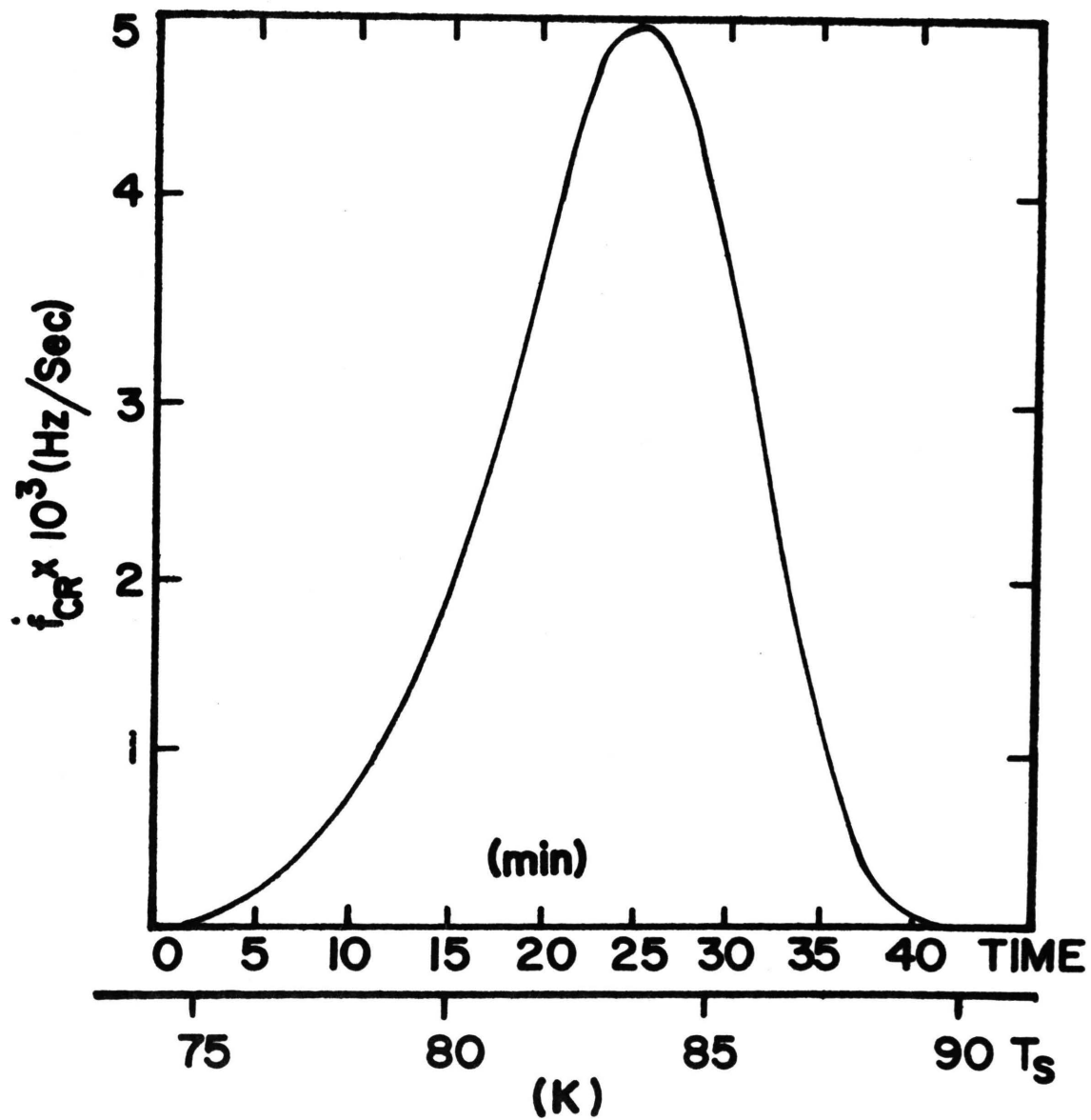


Figure 7. Flash Desorption of CO<sub>2</sub> from an H<sub>2</sub>O Surface



## PART II

Condensation Coefficient Measurements  
of  $H_2O$ ,  $N_2O$ , and  $CO_2$

To be submitted to The Journal of  
Vacuum Science and Technology

Condensation Coefficient Measurements  
of  $\text{H}_2\text{O}$ ,  $\text{N}_2\text{O}$ , and  $\text{CO}_2$

C. E. Bryson, III, V. Cazcarra, and L. L. Levenson

ABSTRACT

A molecular beam was used in conjunction with quartz microbalances to measure the condensation coefficients,  $\gamma$ , of  $\text{H}_2\text{O}$ ,  $\text{N}_2\text{O}$ , and  $\text{CO}_2$ . This ratio,  $\gamma$ , was observed to be a function of the beam temperature, incident flux, and the time that the surface was exposed to the beam as well as the surface temperature. Problems associated with the definition of  $\gamma$  are discussed in attempts to explain the data. The range of  $\gamma$  observed was 0.5 to 0.995.

## INTRODUCTION

The measurement of condensation coefficients provide an important method for studying the condensation process and gas-surface interactions. Even though the literature on this subject is extensive and reflects a large amount of theoretical and experimental work,<sup>(1,2,3)</sup> there is still a need for further work because much of the experimental data taken to date are inconsistent, and the theory is difficult to relate to the physical situation.<sup>(2)</sup> Difficulties lie in two areas. First, the definition of the condensation coefficient itself can be ambiguous. This ambiguity makes comparisons between one experiment and another and between experiment and theory difficult. The other difficulty is the lack of control of the important variables and parameters.

It is frequently convenient to distinguish between the concepts of sticking coefficients and condensation coefficients.<sup>(1)</sup> Both are the ratio,  $\gamma$ , of the rate at which material condenses or sticks on a surface to the rate at which material arrives at or is incident upon the surface. Here, as in reference (1), the sticking coefficient is referred to the situation in which the surface is composed of a different material than the incident material, whereas, the condensation coefficient is referred to the situation in which the surface is composed of the condensed phase of the same material that is incident.

There have been numerous experimental studies and attempts at a theoretical prediction of the behavior of  $\gamma$ . In the various cases of sticking coefficients, some have been satisfactorily explained. Eyring, Wanlass and Eyring were able to explain satisfactorily the sticking of nitrogen to a tungsten surface with a transition rate theory.<sup>(4)</sup> Henning treated reasonably well the sticking of Au on NaCl with a model that was based on a combination of cluster growth and trapping probability.<sup>(5)</sup> We were able to explain the sticking of  $\text{CO}_2$  to an  $\text{H}_2\text{O}$  surface with a nucleation theory.<sup>(6)</sup> In contrast, the results obtained from the measurements of condensation coefficients have been less well understood. Qualitatively, both experimental and theoretical work show that as the surface temperature is lowered the condensation coefficient tends toward unity.<sup>(2)</sup> However, details of this behavior have been elusive, and theoretical treatments have been relatively unsuccessful.<sup>(2)</sup> One notable exception is the treatment of Busby et al.<sup>(7)</sup> of argon data.

The work reported here consisted of an experimental study of the condensation coefficients of  $\text{H}_2\text{O}$ ,  $\text{CO}_2$ , and  $\text{N}_2\text{O}$ . A molecular beam was used to determine the reflection coefficient,  $(1-\gamma)$ , by measuring the rate at which material left a surface. The measurement was made as a function of surface temperature,  $T_s$ , beam temperature,  $T_g$ ,

incident flux,  $D$ , angles of incidence and reflection, and amount of time the surface was exposed to a beam. With the exception of the angles of incidence and reflection, the parameters were controlled and varied over reasonably wide ranges, and a strong dependence of  $(1-\gamma)$  on each was found. The solid angle of the detector and the target surface was rather large, and only two geometries were used. Consequently the dependence of  $(1-\gamma)$  on the angles of incidence and reflection were not determined, although a large dependence was noted. In addition, a study of the sublimation of  $N_2O$  from a  $CO_2$  surface was performed.

The direct application of trapping probability models to our results is not possible because the models<sup>(7,8)</sup> do not contain all the parameters which we experimentally observed to be important. The most serious problem in attempting to use these models is the fact that they do not include the possibility of having one molecule impinge on another molecule that had previously hit the surface and which had not completely lost all attributes of having been a gas molecule. Experimentally, it appears that the molecules on a surface do remain in a higher energy state long enough for this possibility to be very probable. This observation, described in detail below and supported by the study of  $N_2O$  sublimation from a  $CO_2$  substrate, restricts the application of the trapping

model results either to very low fluxes or to the time directly following initiation of the beam. The transition rate approach does not suffer directly from these shortcomings but requires detailed knowledge of the partition functions of the surface.<sup>(4)</sup> Suitable models that would allow the calculations of this partition function are not apparent. Further, there is evidence that the incident molecules accommodate so slowly that  $T_g$  is not defined during the time the beam is on; however, some features of our data can be discussed in these terms in a meaningful way.

Comparisons of the data reported here with earlier measurements are not possible for the same reasons that comparison with the above mentioned theory is not possible. Specifically, either the data obtained in earlier work were not precise or not all of the parameters we observed to be important were monitored.

Previous work, including some initial studies in our laboratory, indicates that any molecules leaving a surface will do so in a diffuse manner.<sup>(9)</sup> This indication led to the simple design of the apparatus which was used in the present experiments. The data we have since obtained show that some molecules may not leave the surface in a diffuse manner. This, coupled with the poor angular resolution of the apparatus, makes detailed analysis of the data difficult. Beyond qualitative explanations of some of the features of the data and some

limited engineering applications, our study should help to define the problem more clearly for future research.

#### EXPERIMENTAL ARRANGEMENT

The apparatus used in our experiments has been described elsewhere<sup>(10)</sup> but will be briefly redescribed here for the reader's convenience. Figures 1 and 2 show the experimental chamber and molecular beam tube surrounded by the cryogen reservoir of a cryostat. The two figures also show the two configurations used. These are referred to as System I and II, respectively. They differ mostly in the angles of incidence and reflection. For our experiments, the cryogen was pumped, solid nitrogen at 50 K. The chambers, which are shown approximately to scale, were 12.5 cm in diameter and 10 cm deep. They contained three microbalances, the molecular beam nozzle, and a 2.5 cm diameter copper disc that served as a target. The chambers and the nozzle communicated with liquid nitrogen, trapped, diffusion pumps through tubes which were connected to the top of the cryostat. The pumping system was provided with a capacitance manometer, ionization gauges, and a General Electric monopole mass spectrometer.

The microbalances were AT-cut, quartz crystal resonators 0.3 mm thick and 1.5 cm in diameter. They had a dominant resonance nominally at 5 MHz. Changes in frequency,  $\Delta f$ , were related to changes in the number of

molecules,  $\Delta n$ , adsorbed per  $\text{cm}^2$  on the microbalances by the expression

$$\Delta n = (1.079 \times 10^{16}) M^{-1} \Delta f, \quad (1)$$

where  $M$  is the gram molecular weight of the adsorbed species.<sup>(11)</sup> Previous measurements have shown that at 50 K at least 99.95 percent of the  $\text{CO}_2$ ,  $\text{N}_2\text{O}$ , or  $\text{H}_2\text{O}$  striking the crystal was adsorbed. In most cases, the rate of change of frequency with time was measured with a Hewlett-Packard 5360 A computer counter and associated electronics.

The dimensions of the beam nozzle were chosen such that the spatial distribution of molecules could be calculated from the cosine law for nozzle pressures below  $10^{-1}$  torr.<sup>(11)</sup> The different dimensions allowed the rate of arrival of materials on the target disc to be calculated from measurements of the frequency of the microbalance marked BM. The beam tube was provided with a heater and a platinum resistance thermometer. The temperature of the beam for these experiments was  $129 \pm 1$  K.

The copper disc used as a target was machined from pure copper, polished, and then vacuum plated with a film of gold about  $1000 \text{ \AA}$  thickness. It was mounted on nylon screws which provided a small thermal leak to the cryogenic bath. Resistance thermometers, germanium and platinum, which were placed in cavities machined into the disc, allowed its temperature to be determined to within 0.1 K.



A comparison of the two thermometers with each other and with temperatures determined by the vapor pressures of nitrogen near 77 K and of solid argon near 50 K confirmed this precision.

The  $\text{H}_2\text{O}$  used for these experiments was doubly distilled and then out-gassed at 100 C for 10 minutes before evacuation. Subsequent mass analysis showed a  $\text{CO}_2$  content of approximately 0.5 mole percent. The high purity  $\text{CO}_2$ , which was commercially available, showed no measurable impurity with the mass spectrometer.

The  $\text{N}_2\text{O}$  was a dry, nominally 98 percent, pure grade gas. Analysis showed the main impurity to be air which was easily removed. This purification was accomplished by repeated evacuation of the bulb in which the  $\text{N}_2\text{O}$  was stored while the  $\text{N}_2\text{O}$  was cooled to 77 K. No impurity could be detected after this procedure was repeated twice. The level of impurity detectability correspond to about 0.01 percent  $\text{O}_2$  in  $\text{N}_2\text{O}$ .

#### PROCEDURE

The experiments were carried out by first cooling the target disc and beam nozzle to preselected values. For  $\text{CO}_2$  and  $\text{N}_2\text{O}$ , the initial target temperature was 50 K. For  $\text{H}_2\text{O}$ , the initial value was 100 K. The initial nozzle temperature was kept constant throughout the particular series of measurements. The higher initial temperature

used for the  $H_2O$  was used because we had observed that the  $CO_2$  contained in the  $H_2O$  did not stick to the disc well, i.e., at least 90 percent was detected at the upper microbalance, marked CR in Figures 1 and 2. Presumably this procedure resulted in a cleaner  $H_2O$  film. At these temperatures, a thick film of the order of  $10^{19}$  molecules  $cm^{-2}$  was deposited with  $D \sim 10^{15}$  molecule  $cm^{-2} sec^{-1}$ .

After the initial film was deposited,  $T_s$  was adjusted to successively higher values. At each value of  $T_s$ , the temperature was stabilized and the beam turned on and off repeatedly. Each time the beam was turned on, a different value of  $D$  was used, and the rate at which the molecules left the surface was monitored by recording  $\dot{f}_{CR}$ , the rate of change of frequency of microbalance CR. The rate at which the material arrived on the target disc surface was determined by monitoring  $\dot{f}_{BM}$ , the rate of change of frequency of microbalance BM. Microbalance BM was located adjacent to the target disc as shown in Figures 1 and 2. A typical recording of  $\dot{f}_{BM}$  vs time is shown in Figure 3.

## RESULTS

Each time the beam was turned on  $\dot{f}_{CR}$  was observed to approach a steady state value that was reasonably reproducible. The reflection coefficient,  $(1-\gamma)$ , was determined from the expression

$$(1-\gamma) = K \frac{\dot{f}_{CR}}{\dot{f}_{BM}} \quad (2)$$

where  $\Delta f_{CR}^{\circ}$  is the difference in the response of the microbalance CR to the rate at which material arrived at the microbalance when the beam was on and off,  $f_{BM}^{\circ}$  is the response of microbalance BM to the incident flux of molecules with the beam on, and K is a geometrical factor. The factor K was determined experimentally. (10)

The data were conveniently examined by plotting  $(1-\gamma)$  as a function of a reduced incident flux, R. In a manner similar to the definition of a supersaturation, R is defined as  $R = D/n_s^{\circ}$  where  $n_s^{\circ}$  is the rate at which material sublimates from the target disc in the absence of an incident flux. Figures 4 and 5 show  $(1-\gamma)$  as a function of R, respectively, for H<sub>2</sub>O and CO<sub>2</sub> as obtained with System I (12). For CO<sub>2</sub>, T<sub>s</sub> varied from 70.0 to 89.1 K, and T<sub>g</sub> was 133 to 152 K for one curve and 256 to 274 K for the other. For H<sub>2</sub>O, T<sub>s</sub> ranged from 138 to 152 K, and T<sub>g</sub> was 275 K. For each surface temperature, D was varied from  $6 \times 10^{12}$  to  $10^{14}$  molecules/cm<sup>2</sup> sec. It can be noted from the figures that most of the data points lie within  $\pm 10$  percent of a smooth monotonic decreasing curve drawn empirically for each value of T<sub>g</sub>. However, the H<sub>2</sub>O data were found to depend on the CO<sub>2</sub> content, and the results presented are for 0.5 mole per cent of CO<sub>2</sub>. Higher impurity levels resulted in higher values of measured  $(1-\gamma)$ .

The measurements of  $(1-\gamma)$  made with System II did not yield results that behave as simply. The data for N<sub>2</sub>O are shown in Figures 6 to 8 and for CO<sub>2</sub> in Figures 9 to 11.

For  $N_2O$ ,  $T_s$  varied from 70 to 83 K. For  $CO_2$ ,  $T_s$  was varied from 76 to 84 K. For each  $T_s$ ,  $D$  ranged from  $3 \times 10^{13}$  to  $2 \times 10^{15}$  molecules  $cm^{-2} sec^{-1}$ . Each figure is for a different  $T_g$ . In contrast to the data obtained with System I, the different curves obtained from the data taken with System II do not all have a common shape. In fact the data is such that a reasonably smooth curve does not describe the results satisfactorily.

The rate at which material left the surface, as represented by  $f_{CR}^o$ , was observed to vary with time after the beam was on. The form of the response, i.e.,  $f_{CR}^o$  vs time, was found to be different for the two configurations and depended on  $T_s$ ,  $T_g$  and  $D$ . For System I and all combinations of  $T_s$ ,  $T$  and  $D$  used, the response of  $f_{CR}^o$  for  $CO_2$  and  $H_2O$  was essentially of the same form as  $f_{BM}^o$ . A similar result was obtained with System II when  $N_2O$  and  $CO_2$  were used and  $R$  was greater than 20.

However, when System II was used with  $N_2O$  and  $CO_2$  and when  $R$  was less than about 20, the response was quite different. When  $R$  was less than 2,  $f_{CR}^o$  exhibited a slow exponential rise. The rise time was longest at the lower values of  $T_s$  but tended to be quite variable and nonreproducible. When  $R$  was between 2 and 20, an overshoot in  $f_{CR}^o$ , as shown in Figure 12, was observed. The magnitude of the overshoot tended to increase with  $T_g$  and was also found to be rather nonreproducible. The size of the overshoot ranged from barely perceptible to those shown in Figure 12.

Because the residual pressure was near  $5 \times 10^{-8}$  Torr, primarily  $N_2$ , the possibility that the nonreproducibility was due to  $N_2$  adsorption was considered. However, the ratio of the pressure of  $N_2$  in the chamber to the saturation vapor pressure of  $N_2$  at the temperature of the surface, was too small for significant  $N_2$  adsorption. This was checked by varying the time between exposures. No correlation with the amount of overshoot and time between exposures was observed.

Another feature of the data that was observed was the slow decay of  $f_{CR}^o$  after the beam was turned off. Time constants for this decay were as long as five minutes and were a function of  $T_s$ . Because the excess sublimation rate was small, i.e., of the order of 10 percent of the normal sublimation rate, this feature was difficult to examine directly. While observing the sublimation of  $N_2O$  from a  $CO_2$  substrate, a similar behavior of the  $N_2O$  sublimation rate was observed. Because the normal sublimation rate of  $CO_2$  was much lower than that of  $N_2O$ , the experiment could be analyzed more clearly. (13)

The experiments were performed by first adjusting  $T_s$  to a stable value, then rapidly depositing a layer of  $10^{15}$  molecules  $cm^{-2}$  of  $N_2O$  on a  $CO_2$  substrate and observing the subsequent sublimation of the  $N_2O$ . A plot of the sublimation rate,  $n$ , vs coverage,  $n$ , showed the desorption to be first order and to represent a constant energy. This was evident from the fact that on a log-log plot the data

fit straight parallel lines that have a slope of unity. Desorption of this type can be described by the equation

$$\overset{\circ}{n} = n\nu \exp(E/RT). \quad (3)$$

The energy of desorption is  $E$ , and  $\nu$  is the frequency factor. Figure 13 shows a plot of  $\overset{\circ}{n}$  vs  $1000/T_s$  for  $n = 3 \times 10^{14}$  molecules  $\text{cm}^{-2}$ . Also shown for comparison, in Figure 13 is the bulk sublimation rate for  $\text{CO}_2$  and  $\text{H}_2\text{O}$ .<sup>(14)</sup> A least square fit to the data represented by the solid line through the data points in Figure 13 yields a value of  $2.9 \pm 0.2$  K cal mole $^{-1}$  for  $E$  and of  $5.4 \times 10^5$  for  $\nu$ . This rather small frequency factor can be interpreted as being the result of a high entropy of the molecules on the surface.<sup>(15)</sup> If it is the free energy that determines the desorption rate, then

$$\nu = \nu_0 \exp\left(\frac{-\Delta s}{R}\right), \quad (4)$$

where  $\nu_0$  is a new frequency factor.<sup>(4)</sup> If one assumes that  $\nu_0 = 10^{13}$ , then  $\Delta s = 19$  cal mole $^{-1}$  K $^{-1}$ . This is not an unreasonable number considering the complexity possible for the molecules and surfaces involved.

From the above discussion, one can see that the behavior of  $\gamma$  with  $T_s$ ,  $T_g$ ,  $D$ , time, and angle is quite complicated. Although none of the theoretical treatments that exist are capable of a complete explanation of these data, some of the features can be qualitatively examined

in terms of different treatments. Part of the difficulty in a direct and more complete application of the theoretical treatments is related to an ambiguity in the definition of  $\gamma$ . In the following discussion, this ambiguity in the definition will be delineated and then certain aspects of the data will be tentatively interpreted in terms of transition rate theory.<sup>(4)</sup>

When there are  $D$  molecules incident on a surface per unit area and per unit time, there are several possible ways to define condensation coefficients with each corresponding to one of the possible courses of events for a particular molecule. For the case of interest here, where the surface is composed of the same molecular species as the incident flux, there are four basic courses of events. These are: 1) The incident molecule hits the surface, completely accommodates, and becomes a surface molecule. 2) The incident molecule hits the surface and desorbs before accommodating completely into the surface. 3) The incident molecule does not hit the surface but hits one of the molecules that has previously hit but has not completely accommodated. 4) The molecule hits the surface and either elastically or inelastically reflects from the surface. It is likely that when the incident molecule hits one of the molecules that is not completely accommodated into the surface, it will have a higher probability of being reflected. If one assumes that the desorption of surface molecules is independent of the presence of an incident

flux, then the  $\gamma$  measured in our experiments includes only those molecules that hit the surface and stay. In contrast, the theories for trapping probability are concerned only with those molecules that hit the surface and reflect either elastically or inelastically. It is not obvious which course of events is included in the transition rate theory as this depends strongly on the model of the surface that is used to calculate the partition function.

One of the most striking features of the data presented here is the difference between the behavior of  $(1-\gamma)$  of  $\text{CO}_2$  as observed with the configuration shown in Figure 1 and that shown in Figure 2. At least two explanations of this difference are plausible. One is that there is a significant specular contribution to the number of molecules that leave the surface. The geometry used in System I is such that any molecules that reflect specularly would not hit the detector microbalance while the geometry used in System II is such that the specular component would hit the detector. The existence of a specular component is in contradiction with the measurements made with the surface temperature high enough that there was not a continual build up of material, that is, none accumulated beyond a possible monolayer.<sup>(16)</sup> This would indicate that for the case here the probability is significant that an incident molecule hits a molecule that has not completely accommodated into the surface with a resultant increase in the probability of a reflection over the probability of



adsorption followed by desorption. If this is the case, the calculation of  $(1-\gamma)$  from the data is in error due to the fact that the coefficient  $K$  shown in Eq. (2) was measured when there was no spectral component. This coefficient could be as much as a factor of 2 high if specular reflection exists. Because the number of molecules leaving the surface will be a sum of those reflecting specularly and those leaving in a diffuse manner, a straight forward correction is not possible. The experiment needs to be repeated with an apparatus capable of making the measurements as a function of angle with high angular resolution. Another possibility is that the structure of the surface depends on the angle of incidence. We have observed for the  $H_2O$  that the specific surface is quite high. A detailed study of surface structure has not been done, so this possibility is still conjectural.

Another striking feature of these data is change in  $(1-\gamma)$  as a function of  $T_g$  when observed with System II. This aspect of the data agrees with what one would expect based on the idea presented by Eyring et al.<sup>(4)</sup> In their work, they showed  $\gamma$  to be the ratio of the rotational partition function of the surface phase to the rotational partition function of the vapor phase. For molecules, one should include the ratio of the vibrational partition functions as a multiplication factor. The ratio of  $(1-\gamma)$  for different  $T_g$ 's taken at fixed  $R$  --  $T_s$  did not change

that much -- should be approximately equal to the ratio of the partition function of the gas phase at the different  $T_g$ . This was observed for  $N_2O$  and  $CO_2$  separately; however, the comparison between  $N_2O$  and  $CO_2$  is not in agreement with what one would expect from the values of the partition function. The partition function calculation predicts that  $(1-\gamma)$  for  $N_2O$  should be higher than for  $CO_2$ , and the reverse is observed. This fact indicates that the partition function of the surface needs to be taken into account.

The calculation of the partition function of the surface phase is complicated by the evidence that the presence of the beam apparently changes the surface. The evidence for this is the fact that the rate at which material leaves the surface as measured with microbalance CR does not fall to the sublimation rate for  $T_s$  immediately after the beam is turned off but decays slowly. For the sublimation of  $N_2O$  from  $CO_2$ , the energy term also is an indication of a beam dependent surface.

#### CONCLUSION

The data reported here indicates that the condensation coefficient can be a complicated parameter that is determined by more than one process on the surface. The condensation coefficient was found to depend on  $T_s$ ,  $T_g$ ,  $D$ , the time the surface has been exposed to the gas and the angles of incidence and reflection. A partial lack of

reproducibility of the results indicates that yet another experimental parameter is important. A more detailed study that includes higher angular resolution and an investigation of other parameters such as those related to surface history is called for. In addition, attention must be paid to the definition of condensation coefficients when comparing different experiments and theories to insure that the same mechanisms or processes are being considered.

## REFERENCES

1. L. Holland, *Brit. J. Appl. Phys.*, 16, 1053 (1965).
2. J. P. Hobson, *J. Vac. Sci. Tech.*, 10, 73 (1973).
3. L. L. Levenson, *J. Vac. Sci. Tech.*, 8, 629 (1971).
4. H. Eyring, F. M. Wanlass, E. M. Eyring, "Condensation and Evaporation of Solids," edited by E. Rutner, P. Goldfinger, and J. R. Hirth, (Gordon and Bresch, New York, 1962).
5. C. A. O. Henning, *Surface Science*, 9, 296 (1968).
6. C. E. Bryson, III, and L. L. Levenson, to be published.
7. M. R. Busby, J. D. Haygood, and C. H. Link, *J. of Chem. Phys.*, 54, 4642 (1971).
8. G. Armand, *Surface Science*, 9, 145 (1968).
9. R. F. Brown, D. M. Trayor, and M. R. Busby, *J. Vac. Sci. Tech.*, 7, 241 (1970).
10. C. E. Bryson, III, V. Cazcarra, M. Chouarain, L. L. Levenson, *J. Vac. Sci. Tech.*, 9, 557 (1972).
11. L. L. Levenson, *Nuovo Cimento, Suppl. Ser.*, 7, 5, 321 (1967).
12. V. Cazcarra, Ph.D. Dissertation, U. of Mo.-Rolla (1972).
13. L. L. Levenson, to be published.
14. C. E. Bryson, III, V. Cazcarra, L. L. Levenson, to be published.
15. J. F. Antonini, *Nuovo Cimento, Suppl. Ser. I*, 5, 354 (1967).
16. C. E. Bryson, III, V. Cazcarra, L. L. Levenson, *J. Vac. Sci. Tech.*, 10, 310 (1973).

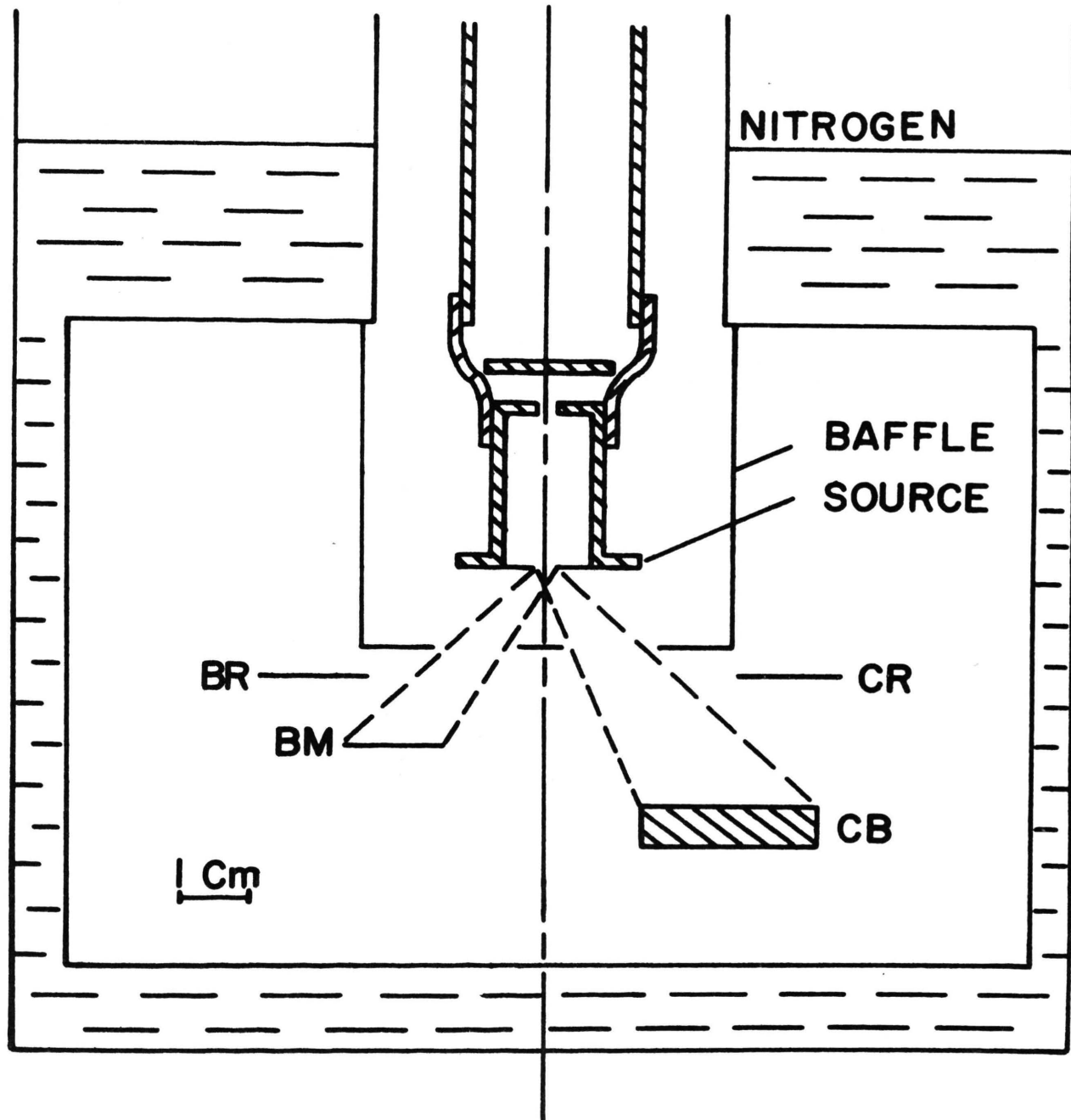


Figure 1. System I.

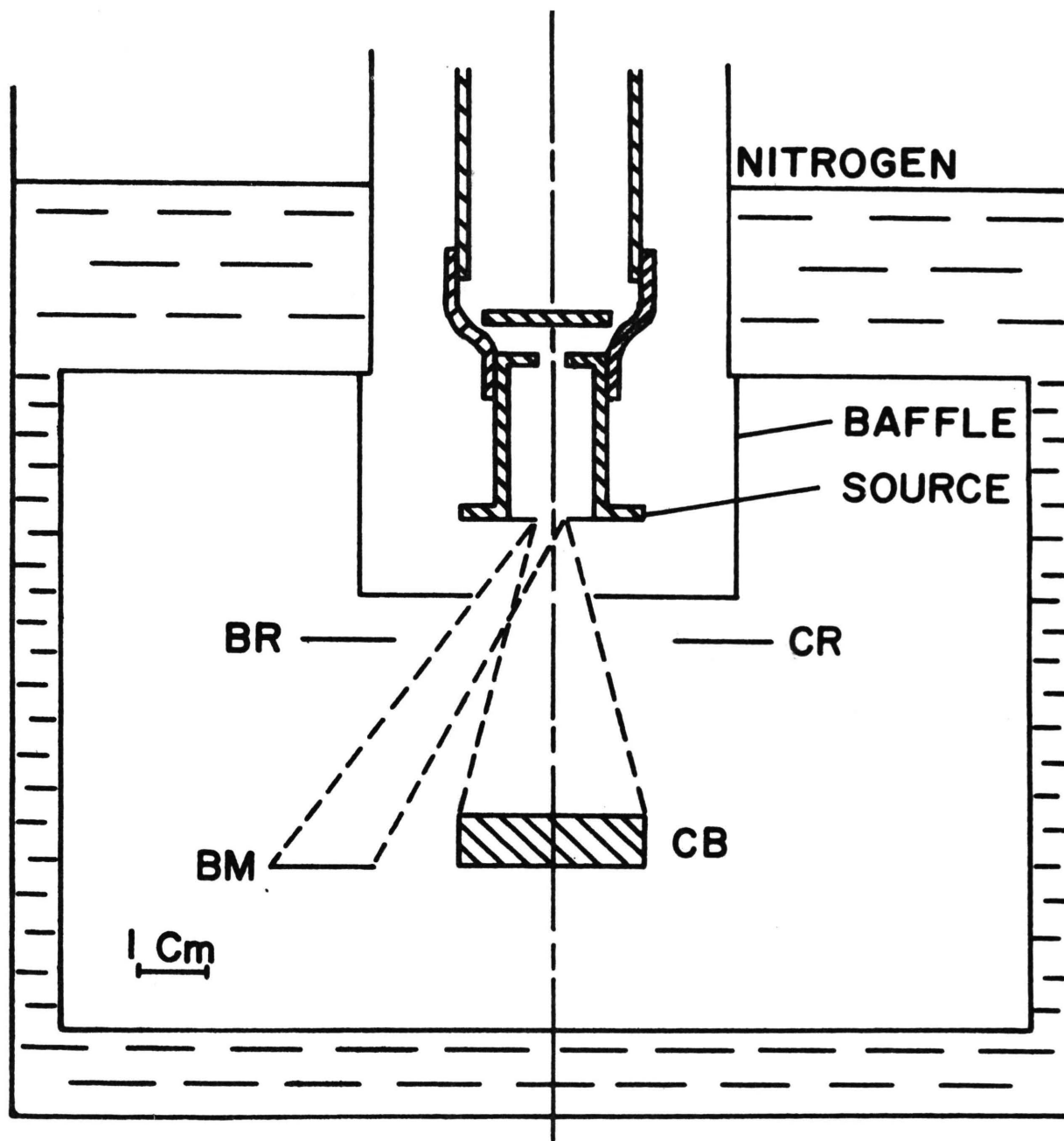


Figure 2. System II.

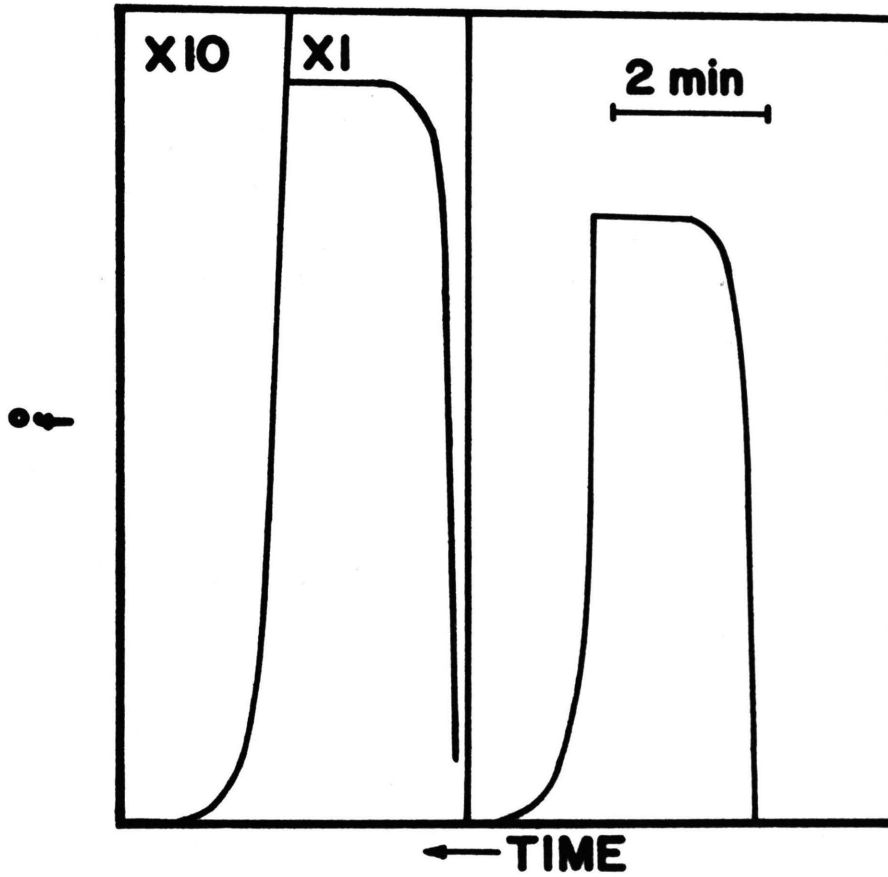


Figure 3. Response of Microbalance BM to a step function in flux.

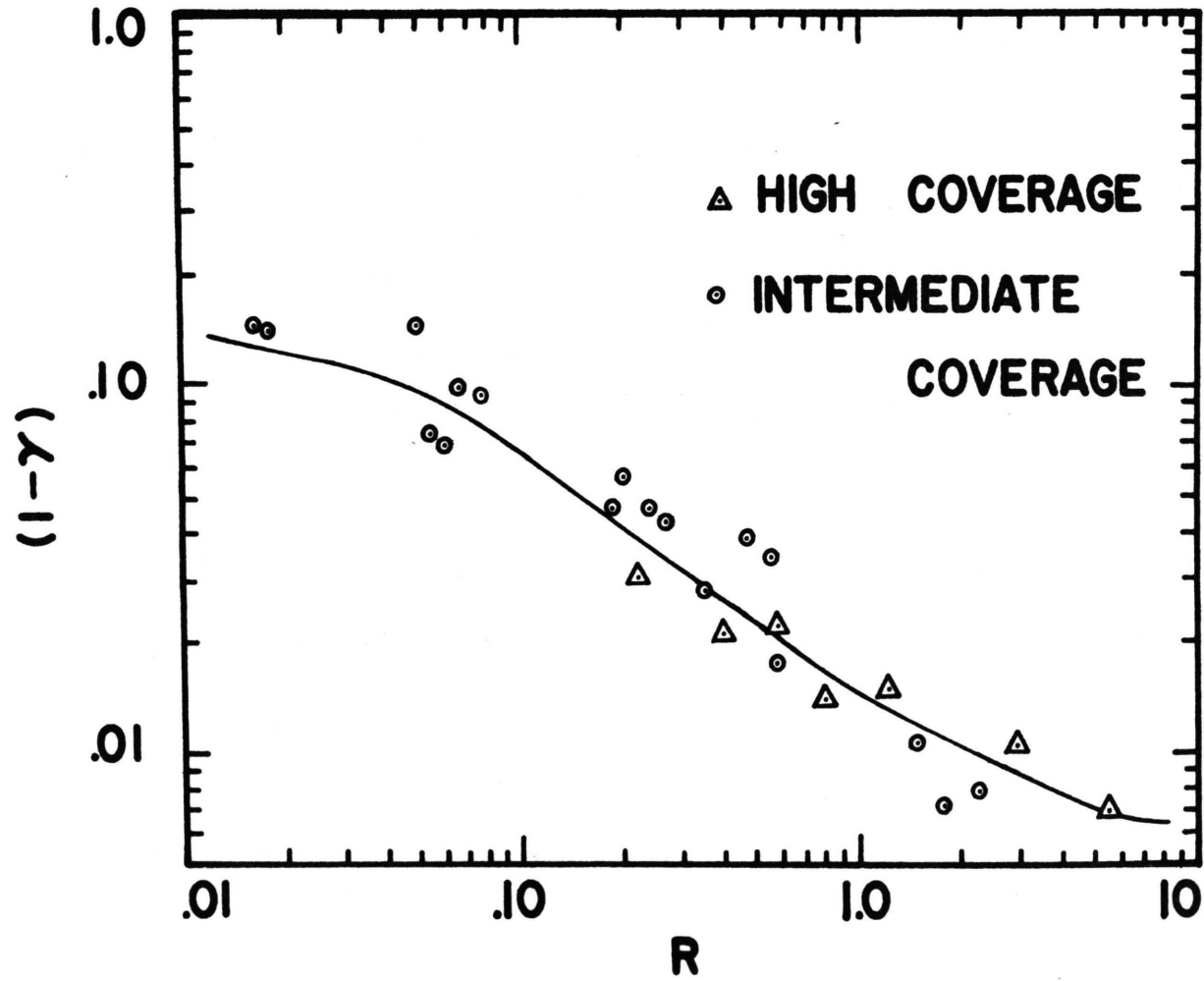


Figure 4. Reflection coefficient as a function of reduced flux for  $H_2O$ , System I



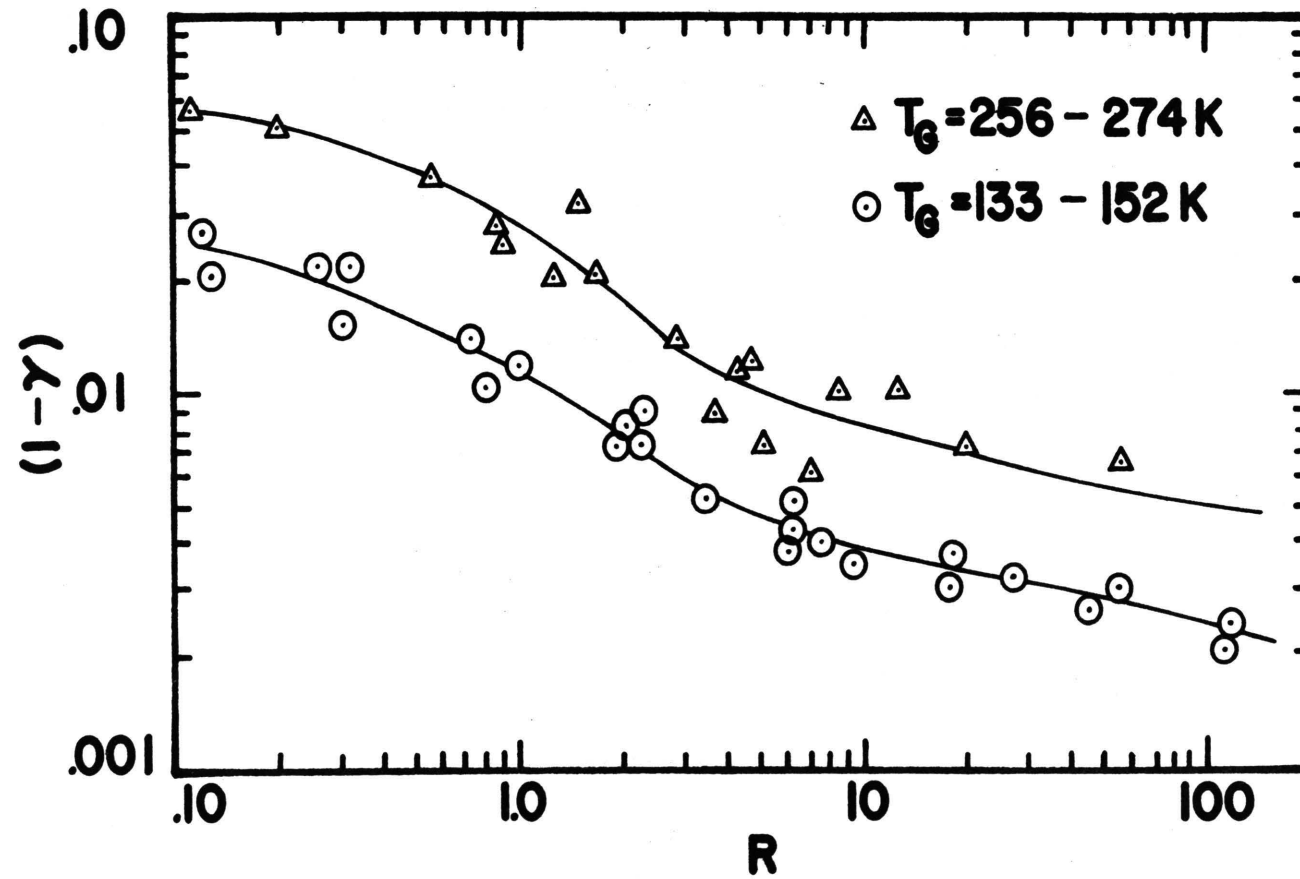


Figure 5. Reflection coefficient as a function of reduced flux for  $\text{CO}_2$ , System I

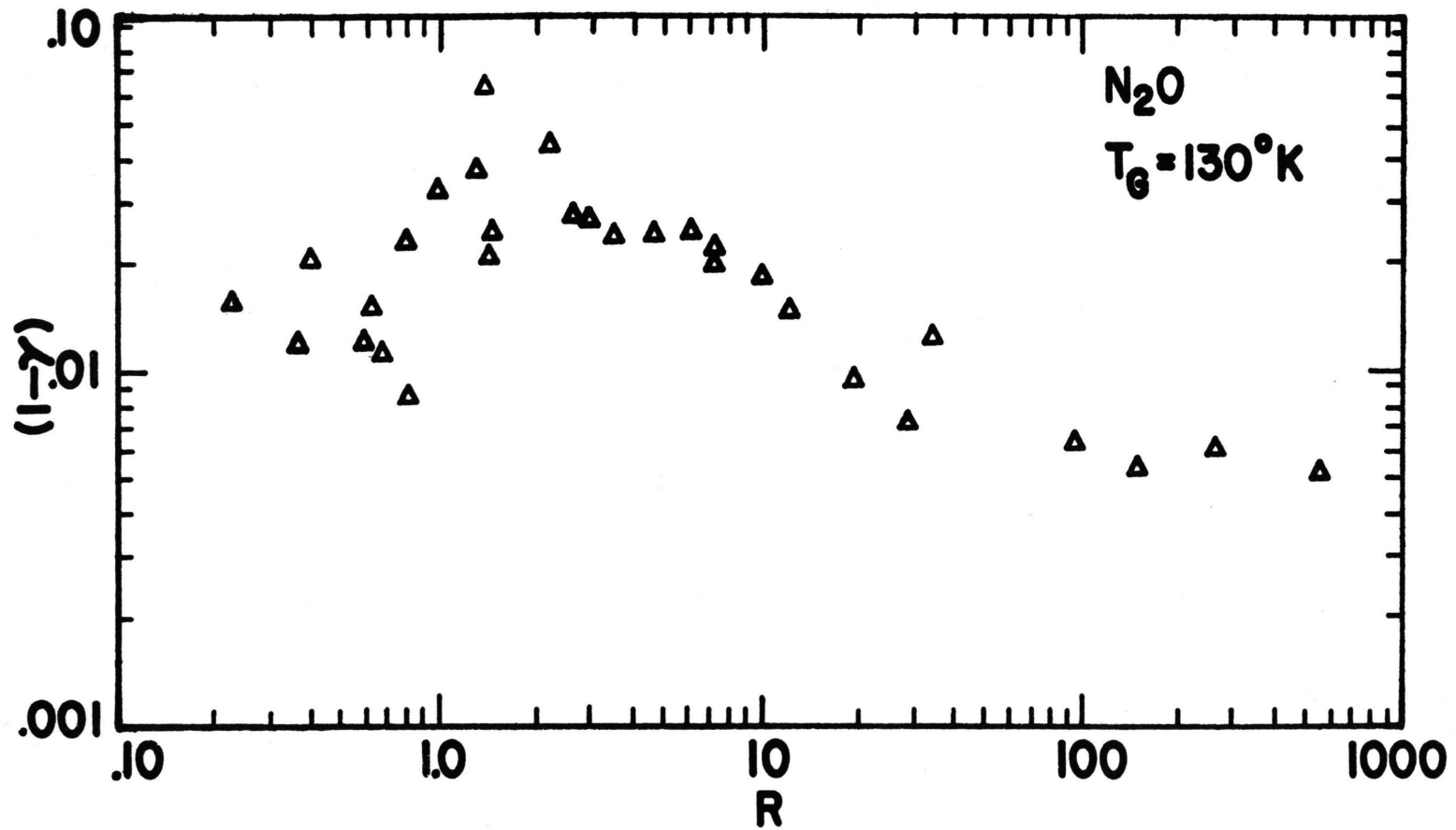


Figure 6. Reflection coefficient as a function of reduced flux for  $N_2O$ ,  $T_G = 130k$ , System II

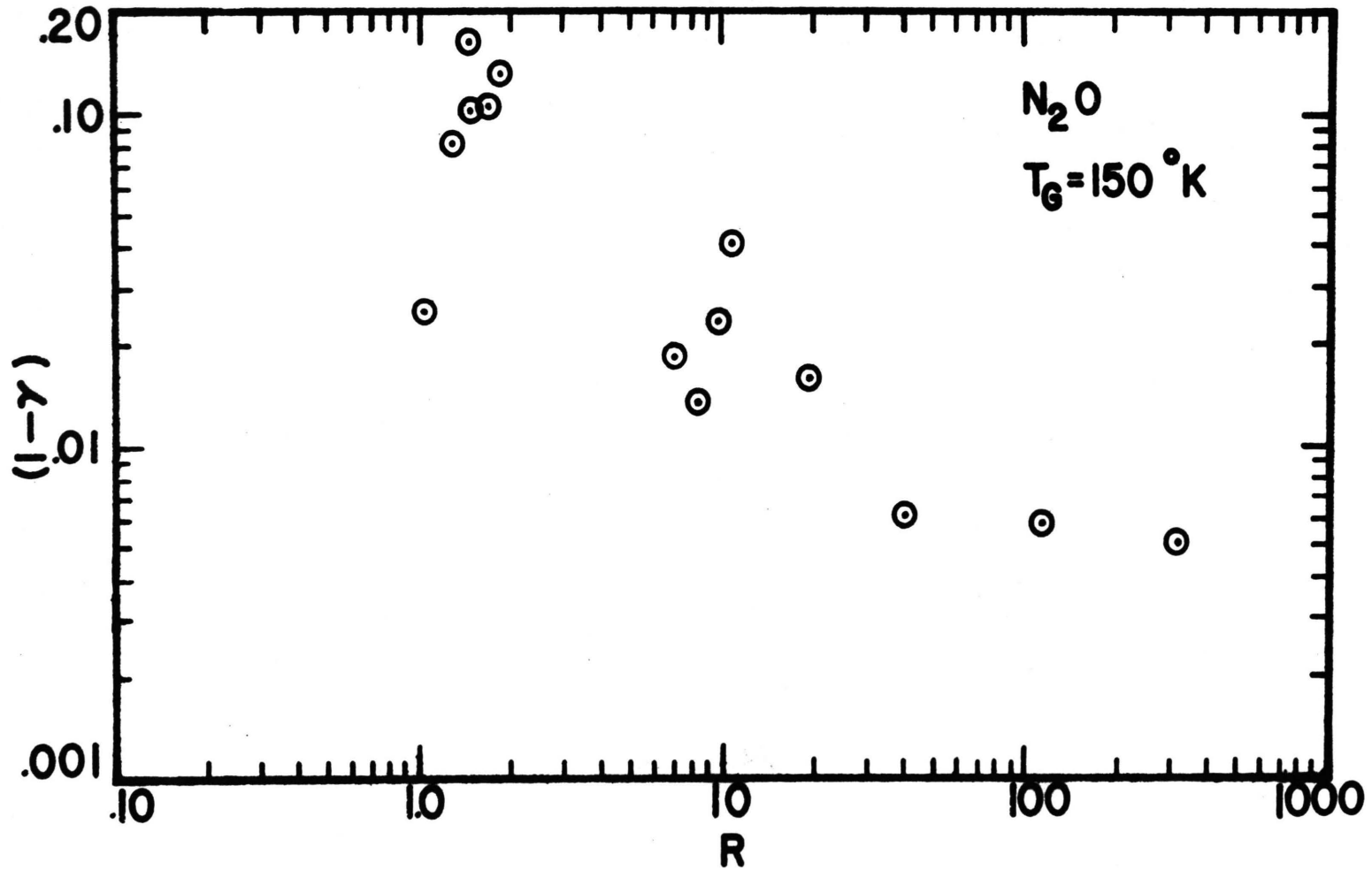


Figure 7. Reflection coefficient as a function of reduced flux for  $N_2O$ ,  $T_G = 150k$ , System II

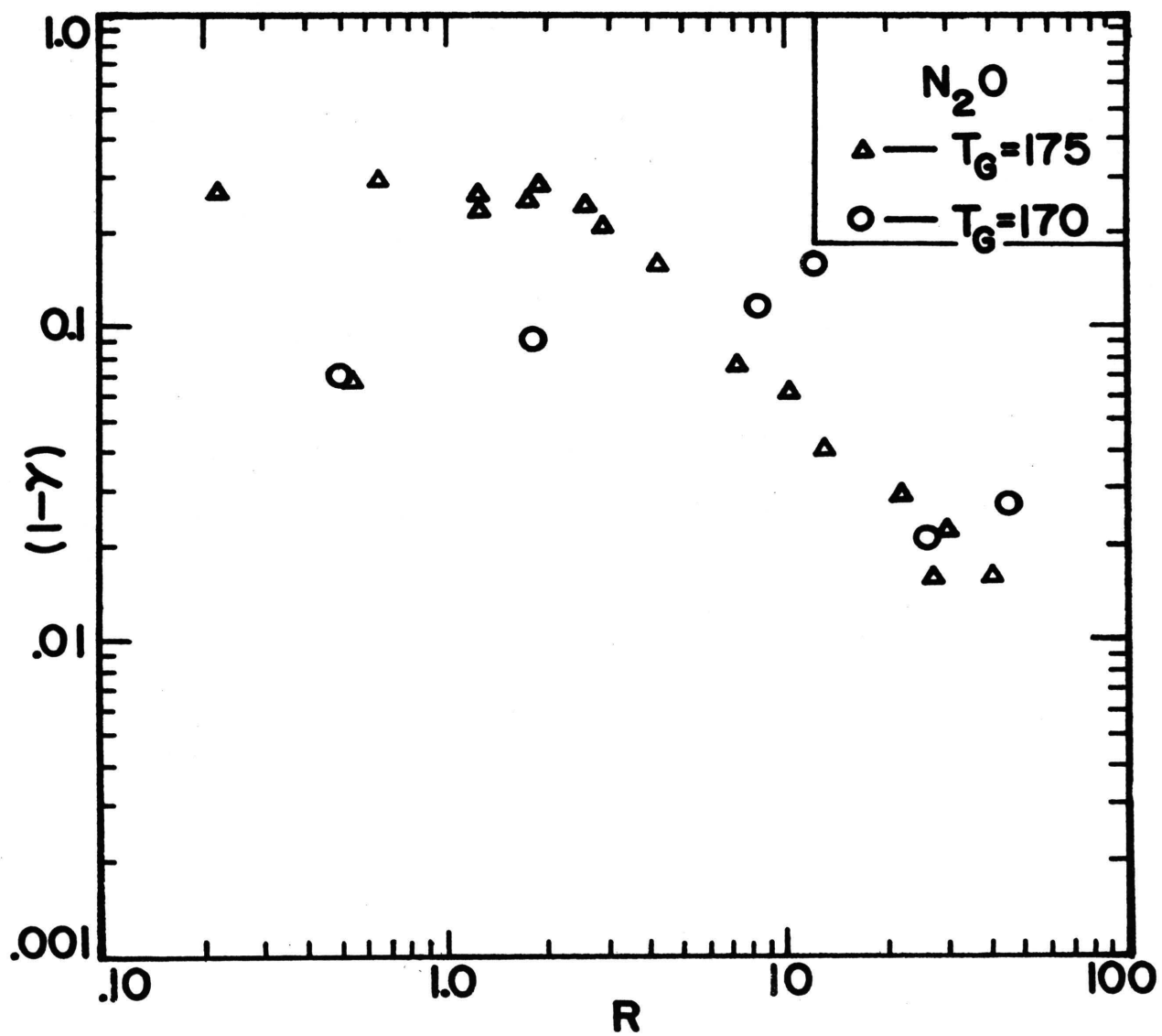


Figure 8. Reflection coefficient as a function of reduced flux for  $N_2O$ ,  $T_G = 170-175k$ , System II

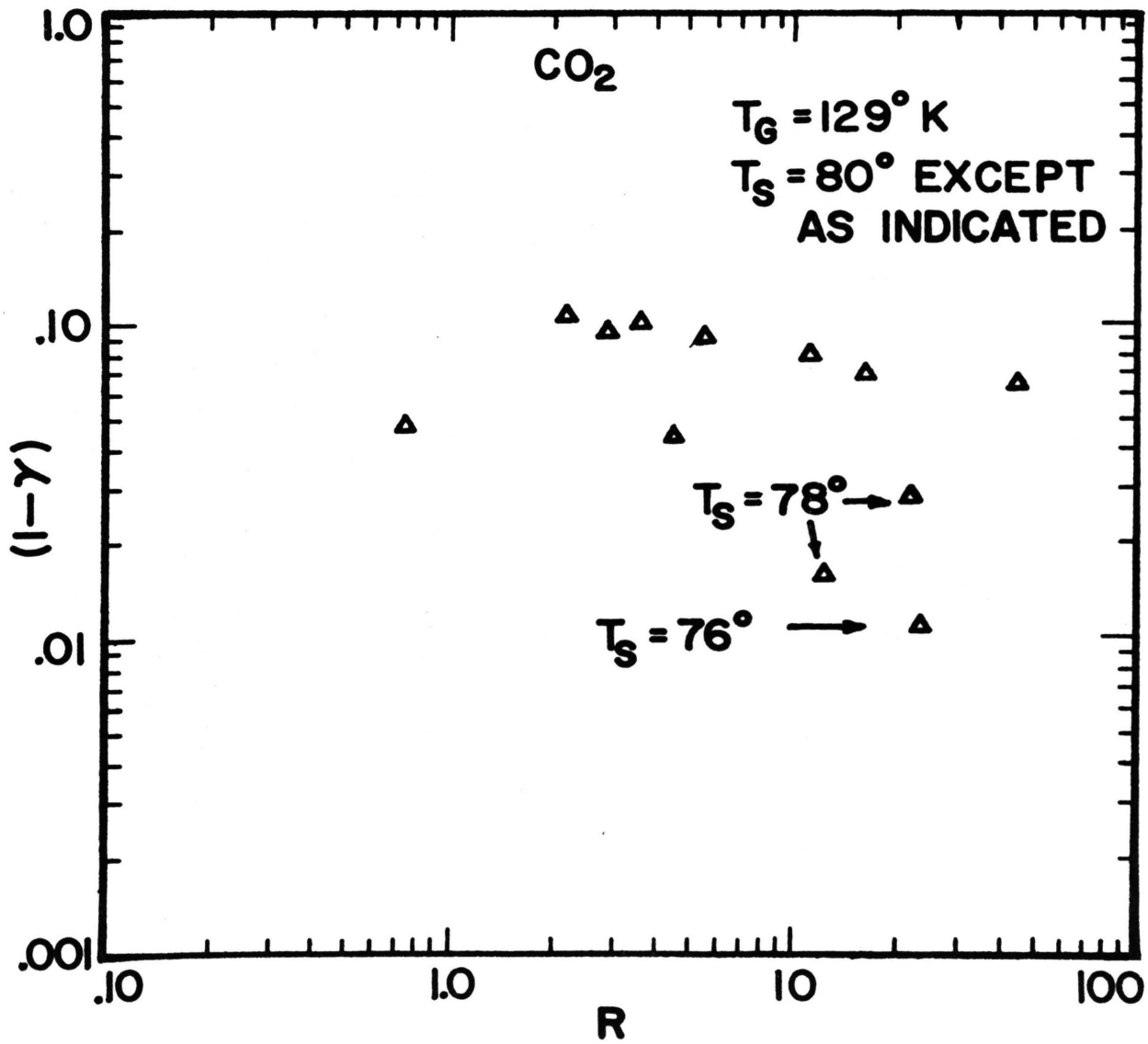


Figure 9. Reflection coefficient as a function of reduced flux for CO<sub>2</sub>,  $T_G = 129\text{k}$ , System II

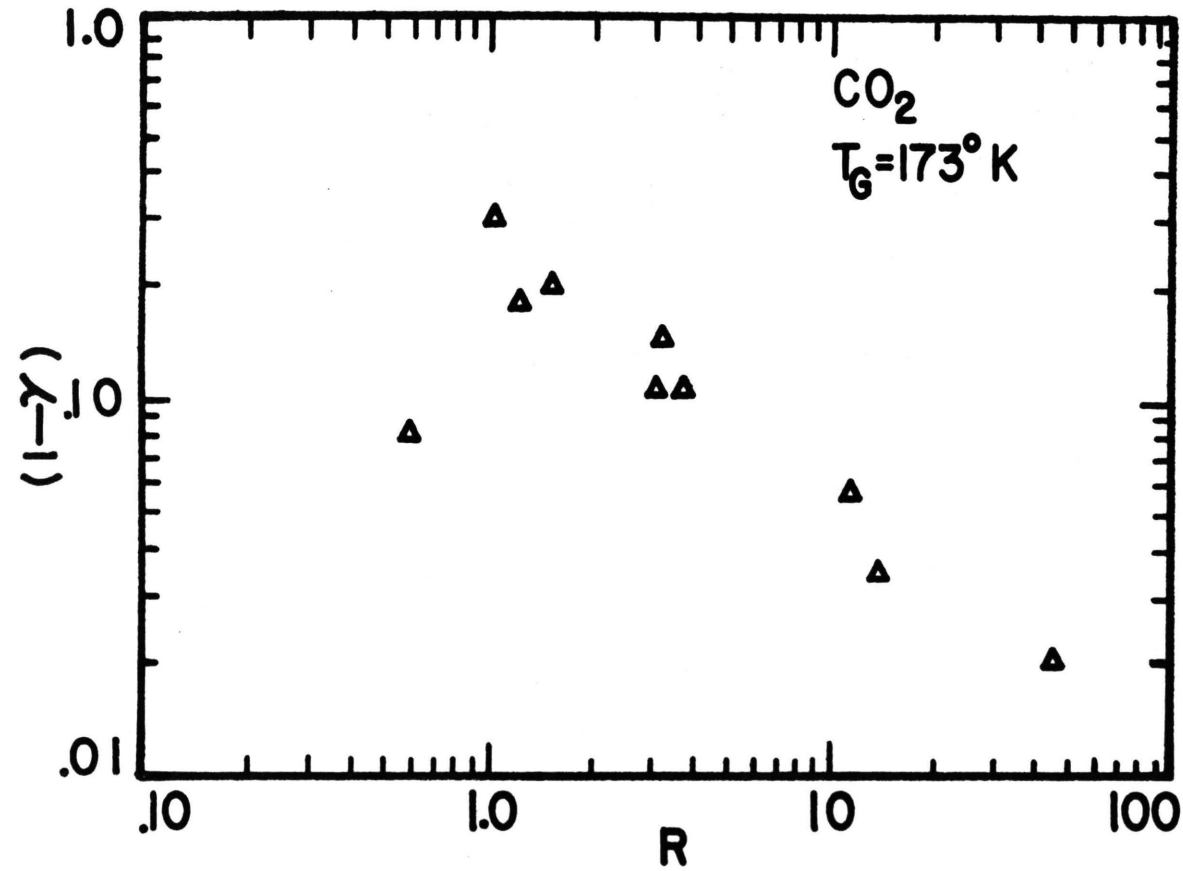


Figure 10. Reflection coefficient as a function of reduced flux for CO<sub>2</sub>, T<sub>G</sub> = 173k, System II

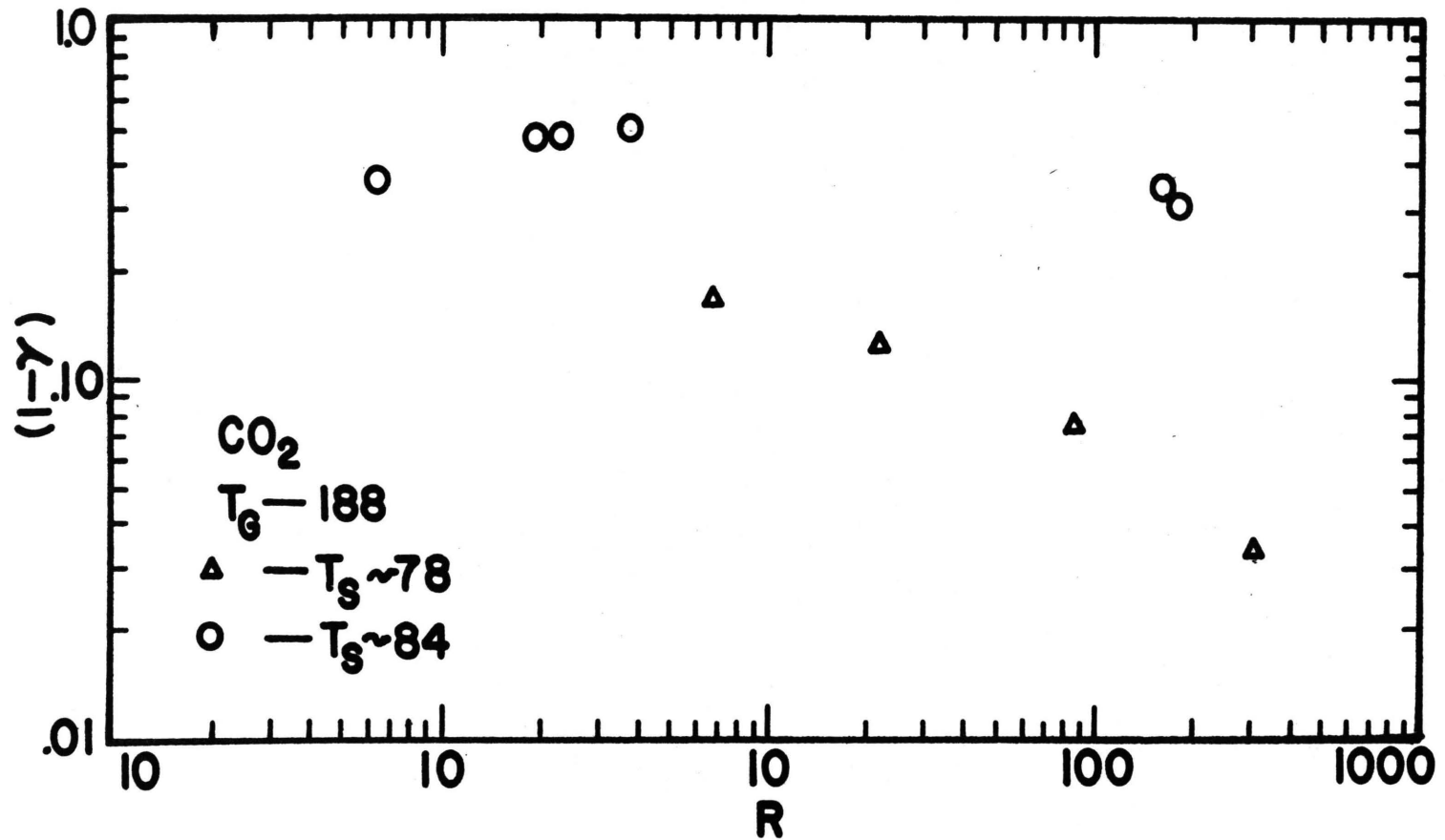


Figure 11. Reflection coefficient as a function of reduced flux for CO<sub>2</sub>,  $T_G = 188k$ , System II

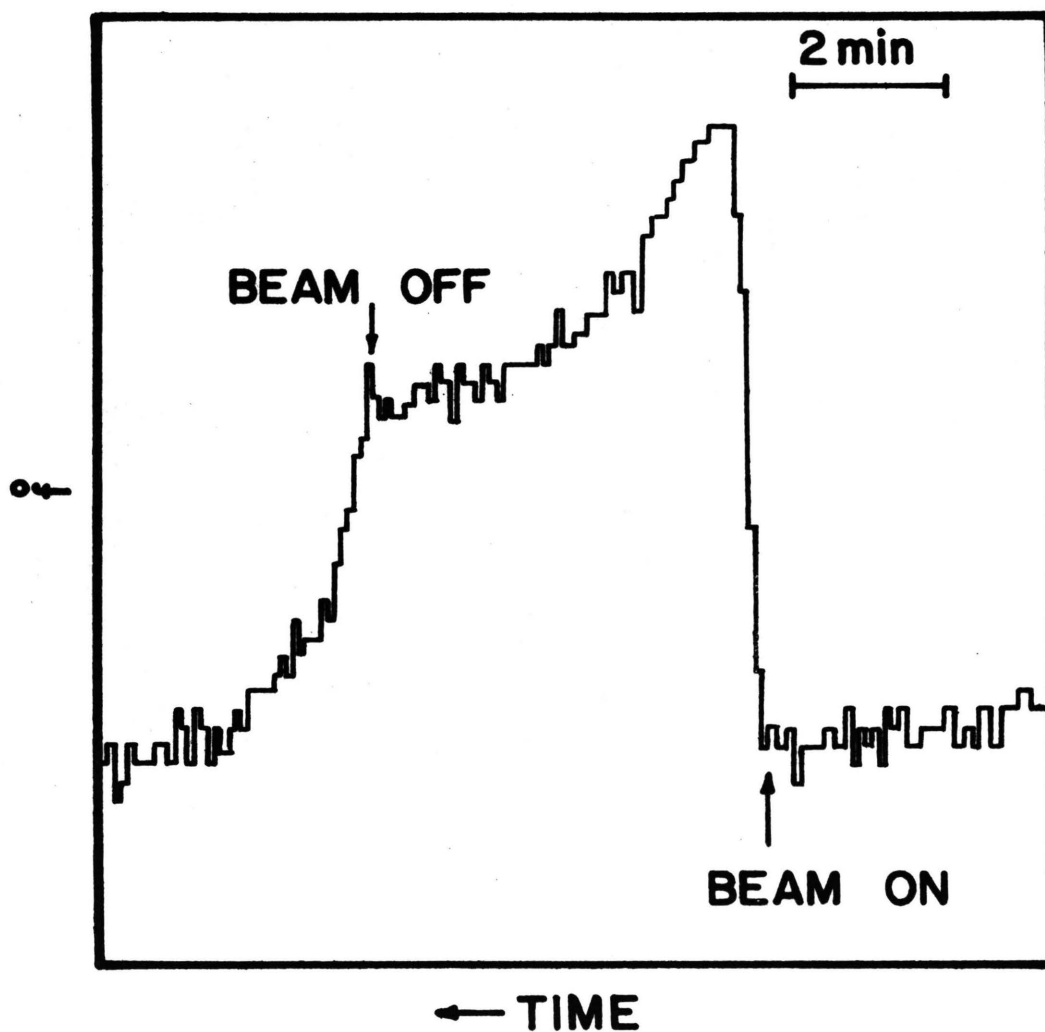


Figure 12. Response of microbalance CR to a step function in flux onto the target.



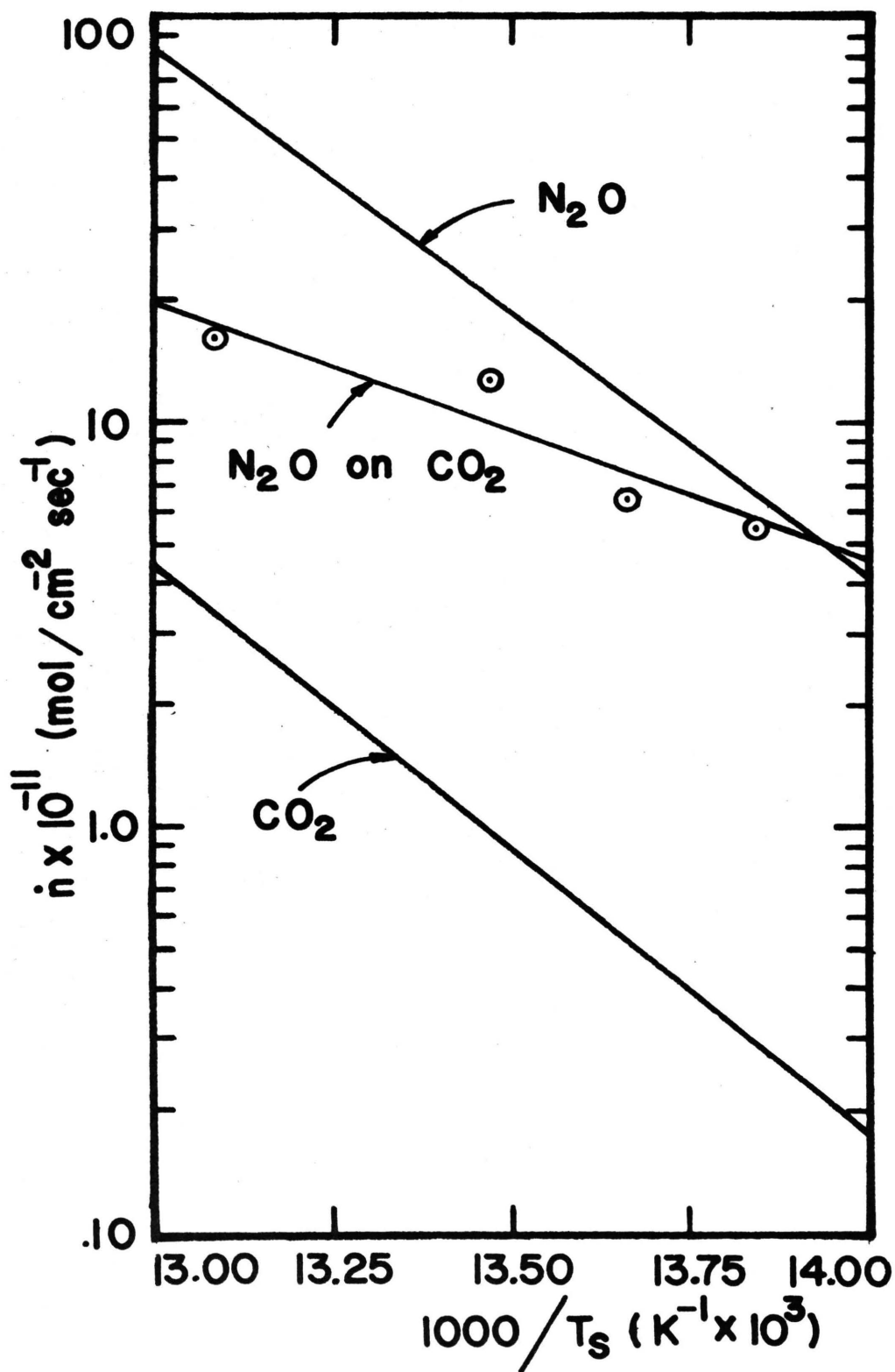


Figure 13. Sublimation rate for N<sub>2</sub>O on a CO<sub>2</sub> substrate and bulk sublimation rate for CO<sub>2</sub> and N<sub>2</sub>O

## PART III

Sublimation Rates and Vapor Pressures  
of  $\text{H}_2\text{O}$ ,  $\text{CO}_2$ ,  $\text{N}_2\text{O}$ , and Xe

Manuscript to be submitted to  
The Journal of Physical Chemistry

Sublimation Rates and Vapor Pressures  
of H<sub>2</sub>O, CO<sub>2</sub>, N<sub>2</sub>O, and Xe

C. E. Bryson, III, V. Cazcarra, and L. L. Levenson

ABSTRACT

The sublimation rates of H<sub>2</sub>O, CO<sub>2</sub>, N<sub>2</sub>O and Xe have been measured in the temperature ranges that correspond to vapor pressures between 10<sup>-4</sup> and 10<sup>-9</sup> Torr. The data, obtained with a quartz crystal microbalance, are compared with existing data and extrapolations. Some of the limitations of the technique are discussed.

## INTRODUCTION

The quartz crystal microbalance has proved to be a useful tool to use in conjunction with the Langmuir free evaporation technique for measuring vapor pressure<sup>(1,2)</sup>. Its mass sensitivity allows the measurement of sublimation rates,  $n$ , that correspond to vapor pressures less than  $10^{-9}$  Torr. Direct measurements in this region of pressure are somewhat limited both by the need for transpiration effect corrections and calibration problems<sup>(3,4)</sup>. The free evaporation technique used with a quartz crystal microbalance circumvents this problem completely.

In the work reported here, this technique was used to measure bulk sublimation rates for  $\text{CO}_2$ ,  $\text{N}_2\text{O}$ ,  $\text{H}_2\text{O}$ , and Xe. The data are compared to the extrapolations of Honig and Hook<sup>(5)</sup> and serve as an effective test of the accuracy of the extrapolations. For these measurements, the microbalances were used to detect a fraction of the molecules leaving a nearby surface. A more direct method is to measure the rate at which molecules leave the surface of a microbalance<sup>(2)</sup>. The latter technique is more sensitive but is not suitable for measurements where the temperature is varied with time. In addition, accurate surface temperature measurements are more difficult.

## APPARATUS AND PROCEDURES

Because the apparatus used for these measurements is described in detail elsewhere<sup>(6)</sup>, only the pertinent aspects are reviewed here for convenience.

The microbalances were mounted near a thermostated target disc in a high vacuum chamber. The chamber was suspended in a 50 K pumped nitrogen bath. The target disc was manufactured out of pure copper, and its temperature was determined to within  $\pm 0.1$  K with Pt and Ge resistance thermometers. A molecular beam was used to deposit a thick film of the molecules to be studied on the target disc. The temperature of the disc,  $T$ , was held near the bath temperature for the deposition of the  $\text{CO}_2$ ,  $\text{N}_2\text{O}$ , and Xe. For the deposition of the  $\text{H}_2\text{O}$ ,  $T$  was held near 100 K. A microbalance located beside the disc and in the beam was used to determine the population density,  $N$ , of the film. For the bulk sublimation measurements,  $N$  was greater than  $10^{19}$  molecules  $\text{cm}^{-2}$ .

A microbalance located above the disc and outside of the incident beam was used to intercept a fraction of the molecules leaving the disc. This fraction could be determined with a precision of  $\pm 20$  percent from the geometry. It was assumed that the molecules left the surface in a diffuse manner<sup>(7,8)</sup>. Comparisons of high sublimation rates with data obtained with conventional pressure measurement techniques showed an agreement of

$\pm 3$  percent.

Previous measurements of the condensation coefficient with this apparatus have shown that, for  $\text{CO}_2$ ,  $\text{H}_2\text{O}$ ,  $\text{N}_2\text{O}$ , and Xe, 99.9 percent of the molecules that hit a 50 K surface remain there<sup>(9)</sup> when the gas temperature is 130 K for  $\text{H}_2\text{O}$ ,  $\text{CO}_2$ , and Xe and 270 K for  $\text{H}_2\text{O}$ .

The molecular beam used to deposit the films was equipped with a monopole mass spectrometer. The gases used were analyzed prior to deposition. The  $\text{CO}_2$  and Xe were commercially prepared, were of high purity grade, and showed no measurable impurities. As purchased, the  $\text{N}_2\text{O}$  was a dry, nominally 98 percent, pure grade gas. Analysis showed the main impurities to be  $\text{O}_2$  and  $\text{N}_2$  in the same proportions as found in air, which were easily removed. This purification was accomplished by repeated evacuation of the bulb in which the  $\text{N}_2\text{O}$  was stored, while the  $\text{N}_2\text{O}$  was cooled to 77 K. No impurity could be detected after this procedure was repeated twice. The level of impurity detectability corresponded to about 0.01 percent  $\text{O}_2$  in  $\text{N}_2\text{O}$ .

The  $\text{H}_2\text{O}$  proved to be more difficult to clean. After starting with doubly distilled  $\text{H}_2\text{O}$  and outgassing it for 10 minutes at 100 C, the  $\text{H}_2\text{O}$  still contained nominally 0.5 mole percent  $\text{CO}_2$ . It was observed that at least 90 percent of this  $\text{CO}_2$  did not stick to the target disc when the  $\text{H}_2\text{O}$  was deposited with the disc held at 100 K. The resulting  $\text{H}_2\text{O}$  film contained less than 0.05 percent  $\text{CO}_2$ .

## DATA TREATMENT

If there are  $n$  molecules  $\text{cm}^{-2}\text{-sec}^{-1}$  leaving a bulk surface and none are incident, the Langmuir vapor pressure,  $P_L$ , (Torr) can be given by

$$P_L = (2.82 \times 10^{-23}) (M T)^{1/2} n$$

where  $M$  is the gram molecular weight of the vapor. The equilibrium vapor pressure,  $P_s$ , is related to  $P_L$  through the Langmuir sublimation coefficient,  $\alpha_L$ , by the expression  $P_L = \alpha_L P_s$ . Although typically near unity, the range of possible values of  $\alpha_L$  is 0 to 1.0. (12)

It can be shown that at equilibrium,  $\alpha_L$  is equal to the condensation coefficient,  $\gamma$ . The coefficient  $\gamma$ , is defined here as the ratio of the number of molecules incident on a surface that stick to the number incident. Experimentally, we have found  $\gamma$  to be a function of the surface temperature,  $T$ , the temperature of the incident molecules,  $T_g$ , the incident flux,  $D$ , the angles of incidence and reflection,  $\alpha_1$ ,  $\alpha_2$  and the time,  $t$ , that the surface has been exposed to the incident flux (6,7). The values obtained experimentally for  $\gamma$  for the molecules used in this study ranged from less than 0.5 to greater than 0.995. A detailed understanding of the behavior of  $\gamma$  as a function of the above parameters is not available at this time, but it has been observed that  $\gamma$  approaches unity as  $T_g$  approaches  $T$ . For the data that are available for those values of  $D$  closest

to  $n$ , for large  $t$  and for the lowest  $T_g$  used for each molecular species,  $\gamma$  was greater than 0.9. Therefore,  $\gamma$  can probably be reasonably assumed to be unity for the situations reported here.

## RESULTS

The data on bulk sublimation of  $H_2O$ ,  $N_2O$ ,  $CO_2$ , and Xe are used in Eq. (2) to calculate the pressure for each temperature listed in Tables I through IV. The data for  $CO_2$  and  $H_2O$  are from Ref. 7. Part of the data for Xe is from Ref. 2. Figs. 1-4 show the same data along with the extrapolations of Honig and Hook<sup>(5)</sup>, i.e., the dotted lines. The solid line represents a least squares fit of the data to an equation of the form

$$\ln(P_L) = \Delta H/RT + B.$$

The values obtained for the constants,  $\Delta H$  and  $B$ , are contained in Table V.

There are two sets of constants for  $H_2O$ . One set is for the data for  $T$  above 150 K and the other is for  $T$  below 150 K. This temperature is approximately the transition from ice IX to ice I<sup>(10)</sup>. From the data given here, the heat of transformation for this phase change is  $740 \text{ cal mole}^{-1}$ . Above 150 K, the data for  $H_2O$  agrees very well with the extrapolation of Honig and Hook<sup>(5)</sup>, which is based on pressure data that go down almost to



$10^{-5}$  Torr. Because the data here go above  $10^{-4}$  Torr, the data in the overlap region serves as a check on the geometrical factor introduced to relate the flux of molecules detected at the microbalance to the rate at which the molecules leave the surface.

The agreement of these data with the extrapolations of Honig and Hook for  $\text{CO}_2$ ,  $\text{N}_2\text{O}$ , and Xe is not quite as good as for  $\text{H}_2\text{O}$ . However, the discrepancies are not unduly large considering that the extrapolations are based on data for the pressure range above  $10^{-3}$  Torr. For  $\text{CO}_2$ , the earlier data by Tickner and Lossing<sup>(11)</sup> do fit an extrapolation of our data to the higher pressure range. In all three cases, the data here are lower than the extrapolations. The recent data on Xe by Leming and Pollack<sup>(4)</sup> are also lower by approximately the same amount. On the basis of our data, the extrapolations of Honig and Hook are excellent guides for the approximate prediction of vapor pressure at lower pressures.

Two limitations associated with using the quartz crystal microbalance were encountered in this work. One was the drift in the frequency, which is associated primarily with the temperature drift of the bath. This drift provides a lower limit on the rate of change of mass than can be reliably detected. For  $\text{CO}_2$  and  $\text{N}_2\text{O}$  this corresponds to approximately  $5 \times 10^{-10}$  Torr. The other limitation was that the vacuum chamber had to be at a low enough temperature so that the vapor pressure in the

chamber was much less than the corresponding sublimation rates being measured. In the case of Xenon, a chamber wall temperature near 50 K limited the measurements to above  $10^{-8}$  Torr.

## REFERENCES

1. J. L. Margrave, ed., The Characterization of High Temperature Vapors, (John Wiley and Son, New York, N. Y., 1967).
2. L. L. Levenson, C. R. Academy Science, Paris, 263, 1217 (1967).
3. G. C. Baldwin and M. R. Gaerttner, J. Vac. Sci. Technol. 10, 215 (1973).
4. C. W. Leming and G. L. Pollack, Phys. Rev. B. 2, 3323 (1970).
5. R. E. Honig and H. O. Hook, R C A Review 21, 360 (1960).
6. V. Cazcarra, C. E. Bryson, III, and L. L. Levenson, J. Vac. Sci. Tech. 10, 148 (1973).
7. V. Cazcarra, Ph.D. Dissertation, Univ. Mo.-Rolla, (1972).
8. C. E. Bryson, III, V. Cazcarra, and L. L. Levenson, J. Vac. Sci. Tech. 10, 310 (1973).
9. C. E. Bryson, III, V. Cazcarra, and L. L. Levenson, to be published.
10. N. H. Fletcher, The Chemical Physics of Ice, (Cambridge University Press, 1970).
11. A. W. Tickner and F. P. Lossing, J. Phys. Colloid Chem. 55, 733 (1951).
12. R. C. Paule and J. L. Margrave, op. cit.

TABLE I

Vapor Pressure of H<sub>2</sub>O vs Temperature, T

Temperature (K)	Pressure (Torr)	Temperature (K)	Pressure (Torr)
187.02	$1.48 \times 10^{-4}$	148.50	$4.70 \times 10^{-8}$
186.80	$1.44 \times 10^{-4}$	147.50	$2.65 \times 10^{-8}$
182.64	$6.91 \times 10^{-5}$	146.30	$1.86 \times 10^{-8}$
176.83	$2.33 \times 10^{-5}$	146.30	$1.86 \times 10^{-8}$
174.57	$1.49 \times 10^{-5}$	146.30	$1.58 \times 10^{-8}$
169.20	$5.00 \times 10^{-6}$	144.90	$2.15 \times 10^{-8}$
159.78	$5.78 \times 10^{-7}$	144.90	$2.01 \times 10^{-8}$
159.58	$7.20 \times 10^{-7}$	144.00	$1.05 \times 10^{-8}$
159.50	$7.04 \times 10^{-7}$	144.00	$1.02 \times 10^{-8}$
159.20	$4.39 \times 10^{-7}$	144.00	$9.77 \times 10^{-9}$
159.20	$3.95 \times 10^{-7}$	142.90	$6.67 \times 10^{-9}$
159.00	$3.73 \times 10^{-7}$	142.90	$5.59 \times 10^{-9}$
153.50	$1.16 \times 10^{-7}$	141.10	$4.70 \times 10^{-9}$
153.19	$1.33 \times 10^{-7}$	141.00	$4.42 \times 10^{-9}$
151.10	$8.64 \times 10^{-8}$	141.00	$4.17 \times 10^{-9}$
151.10	$8.64 \times 10^{-8}$	136.90	$2.66 \times 10^{-9}$
151.00	$5.75 \times 10^{-8}$	134.50	$9.28 \times 10^{-10}$
151.00	$5.75 \times 10^{-8}$	134.50	$7.17 \times 10^{-10}$
151.00	$4.99 \times 10^{-8}$	131.80	$6.33 \times 10^{-10}$
149.34	$3.90 \times 10^{-8}$		

TABLE II

Vapor Pressure of  $N_2O$  vs. Temperature, T

Temperature (K)	Pressure (Torr)	Temperature (K)	Pressure (Torr)
80.2	$9.09 \times 10^{-7}$	74.7	$4.75 \times 10^{-8}$
79.8	$4.25 \times 10^{-7}$	74.6	$4.11 \times 10^{-8}$
79.4	$6.66 \times 10^{-7}$	74.5	$3.27 \times 10^{-8}$
79.3	$5.91 \times 10^{-7}$	74.4	$3.57 \times 10^{-8}$
79.0	$3.78 \times 10^{-7}$	74.3	$3.57 \times 10^{-8}$
77.2	$1.78 \times 10^{-7}$	74.3	$3.57 \times 10^{-8}$
77.1	$1.33 \times 10^{-7}$	74.3	$3.13 \times 10^{-8}$
77.1	$1.32 \times 10^{-7}$	74.3	$3.75 \times 10^{-8}$
77.1	$1.66 \times 10^{-7}$	73.9	$3.16 \times 10^{-8}$
77.0	$1.24 \times 10^{-7}$	73.8	$2.58 \times 10^{-8}$
77.0	$1.42 \times 10^{-7}$	73.4	$2.31 \times 10^{-8}$
76.7	$1.69 \times 10^{-7}$	73.3	$1.59 \times 10^{-8}$
76.4	$5.70 \times 10^{-8}$	72.4	$1.06 \times 10^{-8}$
75.8	$9.38 \times 10^{-8}$	71.3	$7.88 \times 10^{-9}$
75.3	$5.66 \times 10^{-8}$	70.3	$2.61 \times 10^{-9}$
75.1	$4.86 \times 10^{-8}$	69.8	$2.59 \times 10^{-9}$
74.8	$6.37 \times 10^{-8}$	68.6	$1.29 \times 10^{-9}$
74.7	$5.55 \times 10^{-8}$	68.6	$1.29 \times 10^{-9}$
74.7	$4.57 \times 10^{-8}$	68.1	$8.55 \times 10^{-10}$

TABLE III

Vapor Pressure of CO<sub>2</sub> vs. Temperature, T

Temperature (K)	Pressure (Torr)	Temperature (K)	Pressure (Torr)
102.50	3.16 x 10 <sup>-4</sup>	77.34	7.09 x 10 <sup>-9</sup>
100.21	1.55 x 10 <sup>-4</sup>	77.22	7.92 x 10 <sup>-9</sup>
98.22	7.92 x 10 <sup>-5</sup>	77.04	8.97 x 10 <sup>-9</sup>
96.15	3.74 x 10 <sup>-5</sup>	77.04	8.96 x 10 <sup>-9</sup>
94.19	1.84 x 10 <sup>-5</sup>	77.04	8.93 x 10 <sup>-9</sup>
91.73	7.49 x 10 <sup>-6</sup>	76.92	8.31 x 10 <sup>-9</sup>
90.00	3.23 x 10 <sup>-6</sup>	76.92	5.13 x 10 <sup>-9</sup>
89.95	3.21 x 10 <sup>-6</sup>	76.92	4.69 x 10 <sup>-9</sup>
89.42	2.87 x 10 <sup>-6</sup>	76.92	4.05 x 10 <sup>-9</sup>
88.97	1.99 x 10 <sup>-6</sup>	76.92	3.99 x 10 <sup>-9</sup>
88.73	2.02 x 10 <sup>-6</sup>	76.86	8.49 x 10 <sup>-9</sup>
88.65	1.91 x 10 <sup>-6</sup>	76.75	4.79 x 10 <sup>-9</sup>
86.91	1.02 x 10 <sup>-6</sup>	76.53	6.00 x 10 <sup>-9</sup>
86.66	7.89 x 10 <sup>-7</sup>	76.28	3.99 x 10 <sup>-9</sup>
85.03	4.13 x 10 <sup>-7</sup>	75.93	4.69 x 10 <sup>-9</sup>
85.00	4.08 x 10 <sup>-7</sup>	75.36	3.47 x 10 <sup>-9</sup>
84.60	2.76 x 10 <sup>-7</sup>	75.13	4.17 x 10 <sup>-9</sup>
84.03	2.46 x 10 <sup>-7</sup>	75.13	4.14 x 10 <sup>-9</sup>
83.96	2.27 x 10 <sup>-7</sup>	75.13	3.95 x 10 <sup>-9</sup>
82.95	1.72 x 10 <sup>-7</sup>	75.13	3.42 x 10 <sup>-9</sup>
81.37	7.61 x 10 <sup>-8</sup>	74.91	2.81 x 10 <sup>-9</sup>
81.37	7.74 x 10 <sup>-8</sup>	74.13	9.98 x 10 <sup>-10</sup>
81.10	5.22 x 10 <sup>-8</sup>	74.02	1.32 x 10 <sup>-9</sup>
80.58	4.98 x 10 <sup>-8</sup>	73.53	8.49 x 10 <sup>-10</sup>
80.00	3.58 x 10 <sup>-8</sup>	73.10	1.33 x 10 <sup>-9</sup>
79.65	3.09 x 10 <sup>-8</sup>	71.99	8.66 x 10 <sup>-10</sup>

TABLE III (continued)

Temperature (K)	Pressure (Torr)	Temperature (K)	Pressure (Torr)
79.36	$2.71 \times 10^{-8}$	71.89	$8.16 \times 10^{-10}$
79.18	$2.50 \times 10^{-8}$	71.84	$6.49 \times 10^{-10}$
79.05	$1.93 \times 10^{-8}$	71.63	$5.38 \times 10^{-10}$
78.62	$1.52 \times 10^{-8}$	71.58	$3.46 \times 10^{-10}$
78.00	$1.34 \times 10^{-8}$	69.69	$8.61 \times 10^{-11}$

TABLE IV

Vapor Pressure of Xe vs. Temperature, T

Temperature (K)	Pressure (Torr)
59.5	$1.03 \times 10^{-6}$
59.3	$9.19 \times 10^{-7}$
58.3	$5.31 \times 10^{-7}$
57.1	$2.34 \times 10^{-7}$
56.7	$1.78 \times 10^{-7}$
53.9	$4.73 \times 10^{-8}$
53.7	$4.48 \times 10^{-8}$



TABLE V

Heat of Vaporization and Preexponential  
for the Data in Tables I-IV

Material	Temp. Range (K)	$\Delta H$ K cal/mole	B ln(Torr)
H <sub>2</sub> O	153-187	12.17 $\pm$ 0.1	24.0
H <sub>2</sub> O	132-153	11.43 $\pm$ 0.3	21.7
N <sub>2</sub> O	68.1-80.2	6.026 $\pm$ 0.1	23.6
CO <sub>2</sub>	69.7-102.5	6.50 $\pm$ 0.1	23.8
Xe	53.7-59.5	3.43 $\pm$ 0.1	15.2

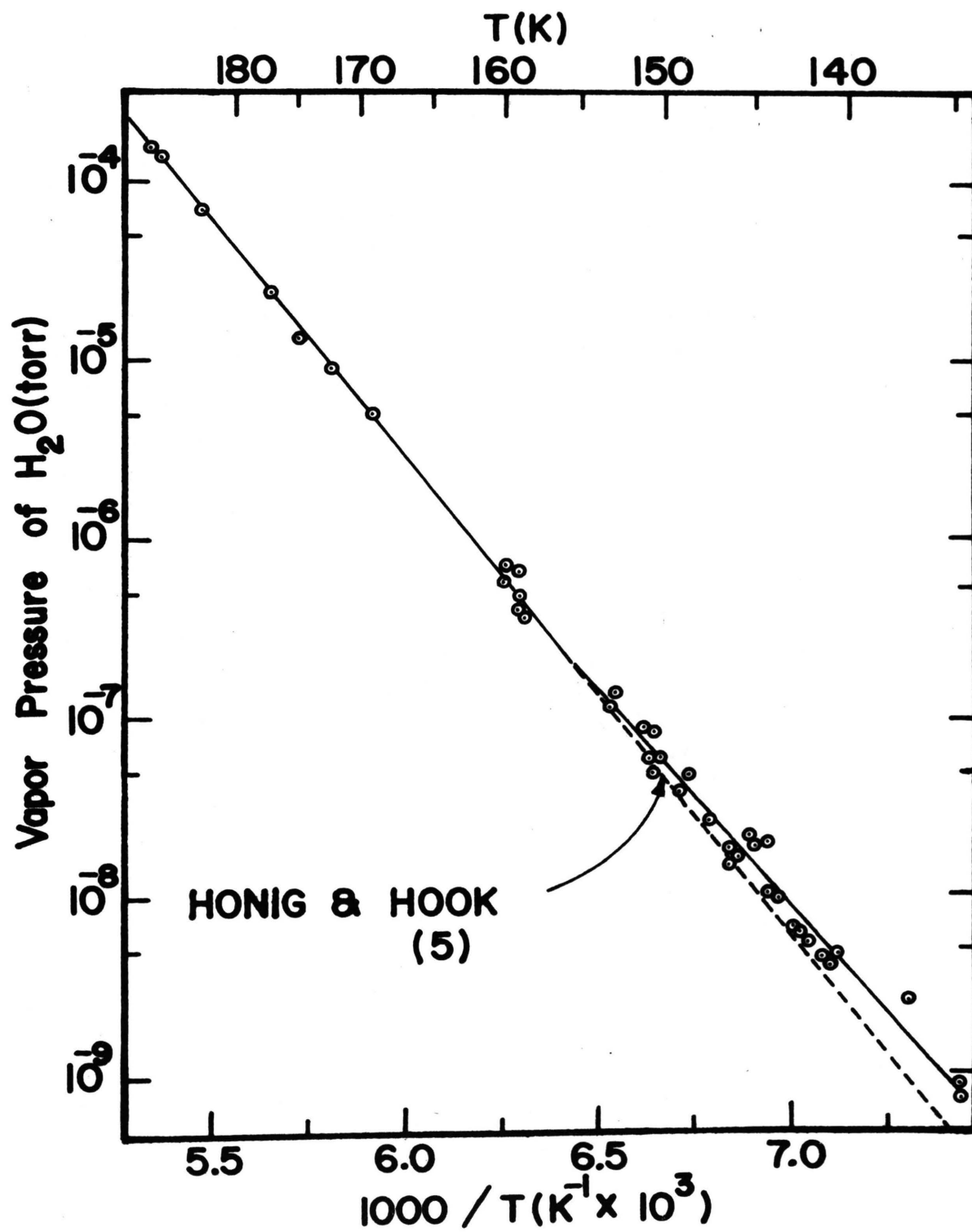


Figure 1. Vapor Pressure of  $H_2O$  vs. Temperature,  $T$

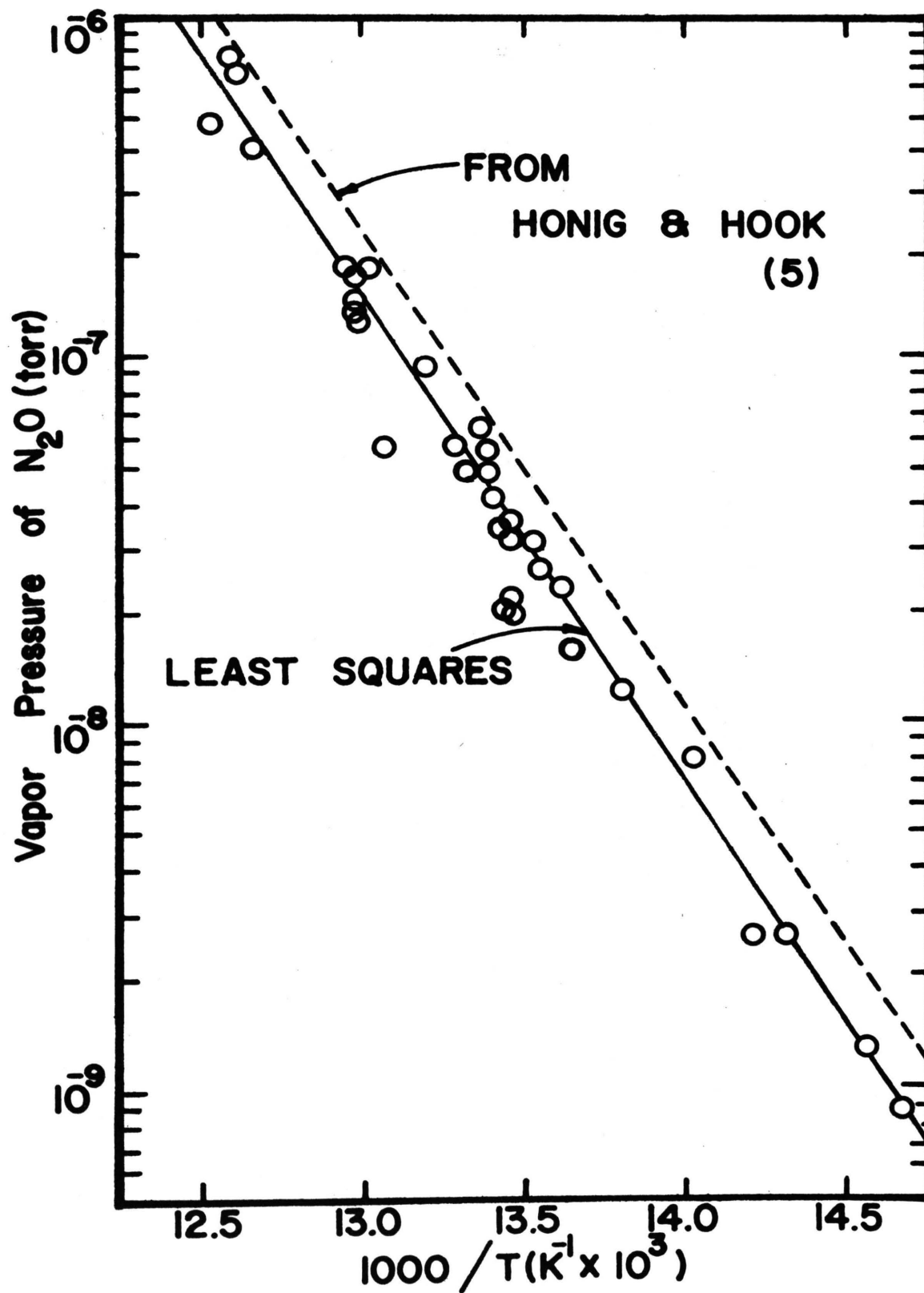


Figure 2. Vapor Pressure of  $N_2O$  vs. Temperature, T

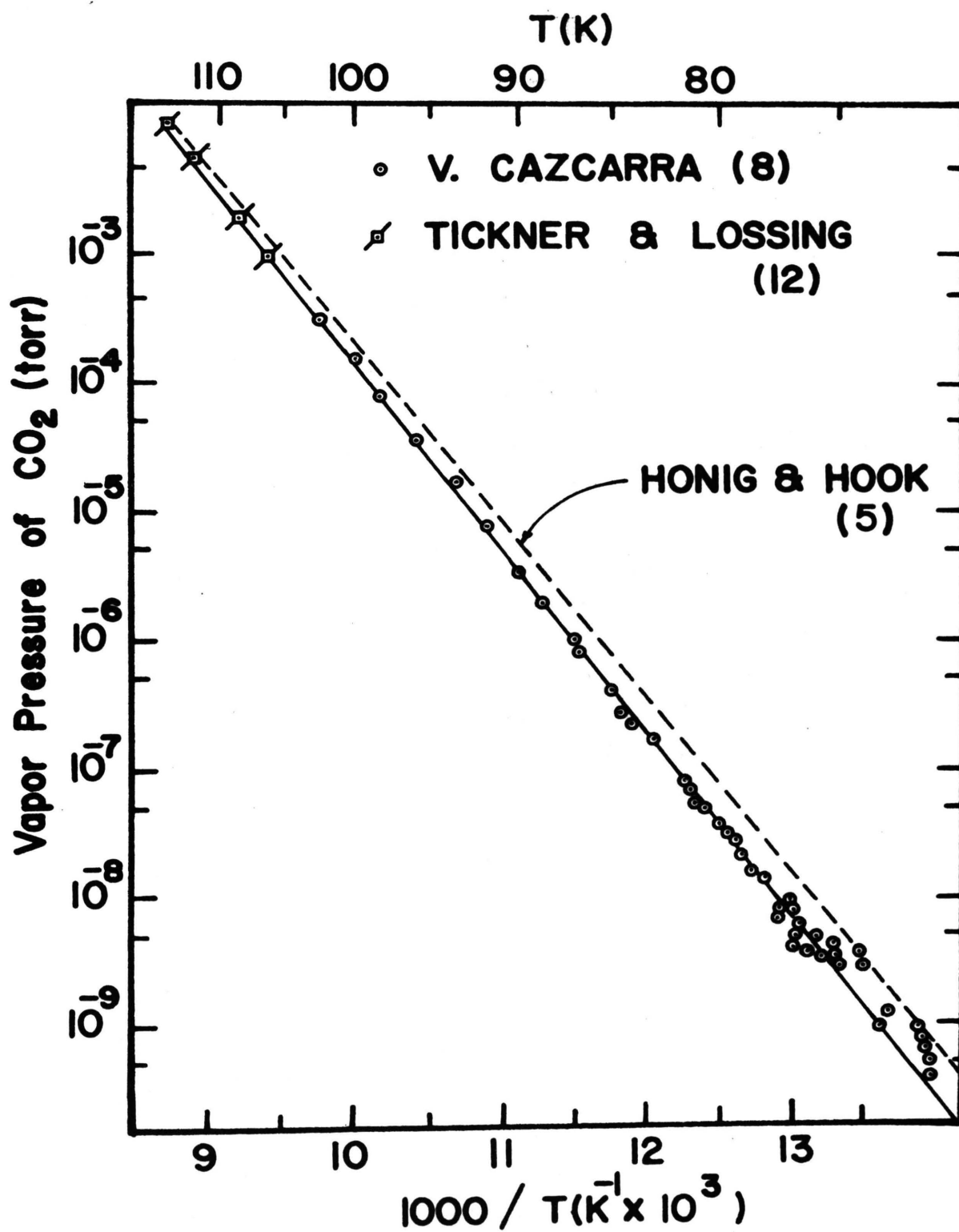


Figure 3. Vapor Pressure of CO<sub>2</sub> vs. Temperature, T

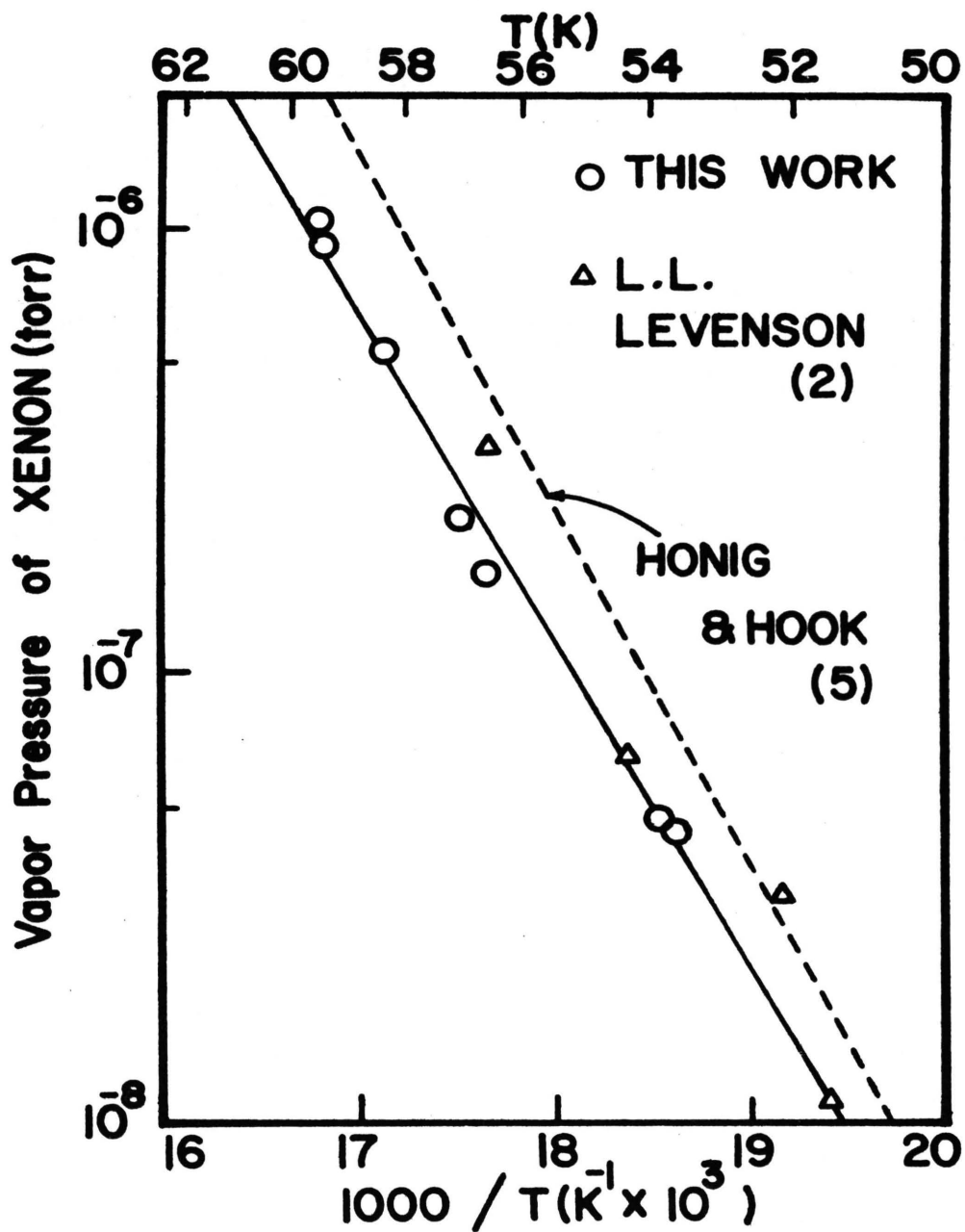


Figure 4. Vapor Pressure of Xe vs. Temperature, T

## VITA

Charles Edward Bryson III was born in Corpus Christi, Texas, September 11, 1940. He entered the U.S. Army in 1958 when he finished high school. He entered Texas A and M University in 1961 and received a B.S. in 1964. He worked as a research engineer for Southwest Research Institute, San Antonio, Texas from 1964 to 1968, and for Technology Incorporated, San Antonio, Texas in 1969. He has worked for the Materials Research Center, UMR, since 1969 as a Senior Electronic Technician. He also entered the graduate school of the University of Missouri-Rolla in 1969 and has since been engaged in graduate research. He is married and has four children.